Forecasting Research

Forecasting Research Division
Scientific Paper No. 27

A Comparison of two vertical grid staggerings.

by

M.J.P. Cullen and J.A. James,
August 1994

Meteorological Office
London Road
Bracknell
Berkshire
RG12 2SZ
United Kingdom

A Comparison of two vertical grid staggerings.

M.J.P.Cullen and J.A.James

August 1994

Forecasting Research Division
Meteorological Office
London Road
Bracknell
Berkshire RG12 2SZ
ENGLAND

Acknowledgements.

The author (J.A.James) would like to thank Dr. B. Golding for his assistance in formulating, executing and analysing the experiments reported in this study, and Dr R.N.B.Smith for help and advice with the boundary layer work.

J.A.James.

Section 1.

Introduction.

A new integration scheme has been proposed for the Unified Model (Cullen, Davies and Mawson (1994)), (hereafter C94). In this proposal it is recommended that the new scheme uses the Charney-Phillips vertical staggering, (potential temperature staggered from the horizontal velocity points), rather than the Lorenz scheme, (potential temperature at the horizontal velocity points). In common with other numerical weather prediction (N.W.P) and global circulation models the current Unified Model uses the Lorenz grid; however a number of recent comparative studies have drawn attention to advantages of the Charney-Phillips grid. For example Arakawa and Moorthi(1987), Leslie and Purser(1992), Fox-Rabinovich (1993), Schneider (1987) and Clarke and Haynes(1993). In particular Arakawa and Moorthi, (hereafter AM) compared the dynamics of a linearized quasi-geostrophic model on the Lorenz and the Charney-Phillips grid and showed that the Lorenz model was subject to spuriously growing short wavelength modes. In the same study it was demonstrated that this spurious amplification of short waves is present in a non-linear hydrostatic primitive equation model; manifesting as noise near the upper and lower boundaries. These spurious short waves can effect larger wavelength modes through non-linear interactions and gravity-wave propagation. In another study Leslie and Purser (1992) showed that the CP grid more accurately reproduces the vertical modes of the linearized hydrostatic Primitive equations, and demonstrated that this advantage is maintained over an ensemble of 100 forecasts from a full hydrostatic primitive equation N.W.P. model.

The improvement in the dynamics demonstrated in these studies is due essentially to the better representation of thermal wind balance and static stability which the staggering of the horizontal wind components and temperature variable allows on the

Charney-Phillips grid. (As discussed in AM and summarised in section 2 of this report).

The development of the Charney-Phillips grid, (Charney and Phillips 1953) was motivated by the wish to satisfy some important integral constraints of quasi-geostrophic flow; for example the conservation of quasi-geostrophic potential vorticity through horizontal advection. The point here is that large scale extra-tropical disturbances are nearly quasi-geostrophic; hence although we may not be interested in making the quasi-geostrophic approximation explicitly in a model we need to establish how important it is that a particular vertical discretization can accurately model these flows.

In contrast, the Lorenz grid (Lorenz 1960) was introduced to facilitate conservation during exchanges between kinetic and potential energy. The conservation of energy is assured through the satisfaction of an exact energy equation in the manner of Arakawa and Suarez (1983). It is the ease with which energy conservation can be enforced that has led to the current popularity of the Lorenz grid.

The difficulty of maintaining energy conservation is an apparent disincentive to using the Charney-Phillips grid. However in C94 it is shown that energy conservation can be ensured in the new integration scheme if a semi-implicit[1] method is used. It is also important to note that the ability to merely conserve energy does not guarantee that we are accurately modelling the relevant physical processes; a point that is illustrated in C94 where it is noted that when the current Unified Model scheme was modified to conserve energy, (in the manner of Arakawa and Suarez), the result was a two degree worsening of the existing cold bias.

---

[1] It may be noted here that the pressure correction equation which is central to the semi-implicit method has a considerably smaller stencil on the Charney-Phillips grid than on the Lorenz.

The emphasis of this report is on comparisons of the dynamics of the two grids. However of considerable importance is the fact that use of the Charney-Phillips grid also has advantages for data assimilation, in that it is easy to calculate balanced height increments to match wind increments. Figure 1 illustrates the error introduced when computing height increments to match given wind increments, and then re-calculating the wind increments from the height increments. A 20% error is typical. This error is a result of the interpolations required by the Lorenz grid, and should not occur on the Charney-Phillips grid where the required balance is easily expressed. (Andrews private communication and Andrews 1993).

The aims of this work are twofold; the models used for the studies of Arakawa and Moorthi and Leslie and Purser cited above, in which the better dynamics of the CP grid were demonstrated, assumed either quasi-geostrophic or hydrostatic balance. The proposed new integration scheme is non-hydrostatic, hence we wish to establish that the improvements will also apply to this formulation. We are also concerned to investigate the effect of the Charney-Phillips staggering on the boundary layer scheme. On the Lorenz grid the variables are positioned conveniently for the calculation of the Richardson number (Ri) and hence for the momentum and temperature diffusion coefficients. On the Charney-Phillips grid however it is necessary to interpolate either u and v, and the momentum diffusion coefficients, or alternatively, theta and the theta diffusion coefficients, (see section 4). This report investigates these alternatives and compares their performance with the Lorenz grid version.

These investigations were carried out through four numerical experiments using a semi-Lagrangian, two time-level version of the "old Mesoscale model" (Golding (1992)). This model has a semi-implicit, semi-Lagrangian, non-hydrostatic formulation, and is therefore similar in its essential aspects to the proposed new Unified Model integration scheme. (Theoretical investigation of

the Charney-Phillips grid is being undertaken within the dynamics group by way of eigen-mode analysis of the linearized non-hydrostatic primitive equations).

A brief discussion of some of the theoretical aspects of the Charney-Phillips and the Lorenz grids is given in section 2. The experiments are introduced, and results presented in sections 3. Finally section 4 presents a summary and discussion.

Section 2.

The Charney-Phillips and Lorenz Vertical Grids.

In this section we summarise some of the important aspects of the Charney-Phillips and Lorenz vertical discretization schemes and anticipate effects on model dynamics. (For a fuller discussion readers are referred to Arakawa 1983 or Arakawa and Moorthi (1987).)

The Charney-Phillips grid was introduced in 1953 as the basis for a vertical discretization of the quasi-geostrophic system of equations. The grid, (figure 2a), holds pressure at the integer levels and vertical velocity and potential temperature, (θ), at the half integer levels (mid layers). It is easy to see that on this grid there are the same number of degrees of freedom in θ as there are in the vertical wind shear. That is for an N layer model there are N degrees of freedom in $\mathbf{v}$, and N-1 degrees of freedom in the vertical shear of $\mathbf{v}$ and θ, hence each value of θ is able to satisfy a thermal wind relation. This situation is in contrast to that on the Lorenz grid (figure 2b), where there is an extra degree of freedom in θ, and consequently in the quasi-geostrophic potential vorticity. This extra degree of freedom gives rise to a spurious computational mode in θ which will not satisfy the thermal wind balance relationship even when it is expected for the continuous case. The extra degree of freedom in the potential vorticity is responsible for the amplifying short modes which are the main disadvantage of the Lorenz grid. (For a discussion of the difficulties of defining and conserving quasi-geostrophic potential vorticity on the Lorenz grid readers are referred to AM).

A complementary perspective on the differences between the dynamics of the Lorenz and Charney-Phillips grids is obtained through consideration of the process of geostrophic adjustment. This process determines the response of a primitive equation

model to departures from geostrophic balance. The departures may be due either to disturbances from forcing processes, or imperfect initial conditions. The transient response of the model consists of the generation of gravity waves which spread out from the centre of the disturbance, to eventually be dissipated throughout the domain. The steady state response after the gravity waves have dispersed is a state of geostrophic balance, the form of which is determined by the comparative scales of the initial disturbance and the Rossby radius of deformation. Considering the vertical momentum equation it is clear that on the Charney-Phillips grid the temperature field is linked to the pressure on the smallest scales. This leads to more accurate calculation of the vertical velocity and better convergence to the hydrostatic balance of the steady state. We may anticipate that the less effective geostrophic adjustment of the Lorenz grid will result in prolonged or increased gravity/inertia wave activity where the solutions are not smooth in the vertical. This is particularly likely to occur at the upper and lower boundaries. Furthermore, as gravity wave amplitudes increase with height so we may expect this situation to be most pronounced at the upper boundary.

Section 3.

The Experiments.

Four experiments are reported in this study. These are:

1. A small scale cold gravity current experiment with no rotational effects.

2. A simulation of the evolution of a two dimensional Eady-Wave.

3. A two dimensional boundary layer evolution study. (The Perth fog case.)

4. A one dimensional boundary layer study. (Wangara Day 33).

The first experiment is a high resolution simulation of a small scale highly non-linear flow. The arguments for the use of the Charney-Phillips grid have all been in terms of improving the treatment of large scale flow features such as balance. This study establishes that any improvement in the larger scale is not gained at the expense of the small scale.

Experiment 2, the simulation of a two dimensional Eady-wave is a study of baroclinic instability; the conditions under which theory and the results of the study by Arakawa and Moorthi suggest improved results may be obtained on the Charney-Phillips grid. The upper and lower boundaries play a particularly important role in this simulation, hence the poorer geostrophic adjustment of the Lorenz grid may lead to increased gravity-inertia wave activity in these areas.

The third experiment is a study of boundary layer evolution. The options for writing the boundary layer scheme on the Charney-Phillips grid are investigated and comparison made with the performance of the Lorenz version.

The final experiment; the one dimensional Wangara boundary layer simulation has been included to provide a further test of the conclusions of experiment 3, but in a simplified setting where the important mechanisms could be more easily identified.

Experiment 1. A Cold Gravity Current.

This experiment was conducted to compare the performance of the two grids on a high resolution small scale problem. The simulation is similar to that of Carpenter et al (1990). A two dimensional domain, (5km high by 16km), is initialised with a cold block of air in the lower left hand corner of an otherwise homogeneous atmosphere. The evolution consists of the descent and subsequent spreading of the cold air along the lower boundary. A number of Kelvin-Helmholtz instability rotors form at the top of the cold air layer. Rigid lid and no change boundary conditions are applied at the upper and lateral boundaries respectively. No surface or boundary layer effects were included and the effects of the earth's rotation are removed. A 5 second timestep was used for all the runs and no artificial diffusion was added to the scheme beyond the slight smoothing characteristic of the third order interpolations used within the semi-Lagrangian method.

The approach of the experiment was simple; a high resolution run is performed as a control and a number of further runs are made with decreasing vertical resolution. Horizontal resolution is kept constant. In this way any divergence between the solutions on the two grids could be assessed.

The relative positions of the levels of the grids as used for this experiment are shown in figure 3; the heights of the temperature levels were matched across the grids as far as possible to ensure that any differences in the solutions were due solely to the staggering of the levels. (This is not possible at the upper and lower boundary, but as a zero gradient in temperature was used as the lower boundary condition, and the upper boundary is relatively unimportant the effect of the difference in the height of these two levels was slight, though possibly visible in the results of the coarsest resolution experiments).

Results from Experiment 1.

The first 750 seconds of the evolution of the control run are shown in Figure 4. At this resolution (Δx=125m, Δz=83m) the solution appears to be essentially grid converged. The impact of decreasing the vertical resolution is shown in figures 5 and 6 which compare the solution on each grid after 500s. It can be seen that the solutions are identical at the higher resolution and that they degrade equally as the resolution is reduced. The slight differences at the lowest level of the coarsest resolution runs do not favour either grid and are almost certainly due to differences in the heights of the lowest temperature levels discussed above.

Conclusions from experiment 1.

We conclude that there is no significant difference between the simulations of this flow obtained from the Lorenz and the Charney-Phillips grid models. This is as expected.

Experiment 2. Two Dimensional Eady-wave Simulation.

This is a simulation of the Eady-wave model of cyclogenesis in which a growing wave forms from a finite perturbation to a baroclinicaly unstable atmosphere. It is under these conditions of baroclinic instability that the different dynamics of the Charney-Phillips and Lorenz grids become apparent, as demonstrated by AM etc. The Eady wave problem has been studied many times in the past; Williams (1967), Simmons and Hoskins (1978), Arakawa(1962), Orlanski(1986), but as far as the authors are aware this is the first study to use the fully non-hydrostatic primitive equations.

The strategy of the experiment is to compare solutions from the Charney-Phillips and the Lorenz grid models with those from Nakamura and Held (1989) (hereafter NH), (figure 7). The NH results were obtained using a hydrostatic primitive equation model and were chiefly concerned with the process of equilibration which occurs after the magnitude of the wave peaks at around day 7. The process of equilibration is complex and in a recent paper, Nakamura (1994), it is suggested that the details are dependant on the form of horizontal diffusion. Since the semi-Lagrangian model has no added diffusion, (and different intrinsic diffusion), we compare results only for the first seven days of the simulation.

This is a two dimensional simulation on an f-plane at 45 degrees North. All the variables are periodic in x with the domain length (L) equal to the wavelength of the initial disturbance. The height of the domain (H) is 10km. The basic state is taken from Williams (1967) and consists of vertically sheared zonal flow in thermal wind balance with potential temperature. The pressure field is in hydrostatic balance with the temperature. All fields are constant in the Y (North-South) direction except potential temperature and pressure. Potential temperature has

a constant North-South gradient and the North-South gradient in pressure is calculated from the requirement of geostrophic balance. The domain, grid dimensions and timestep were;

$L = 4000$ Km, $H = 10000$ m, $\Lambda x = 31250.$ m, $\Lambda z = 240$ m.

$\Lambda t = 100$ seconds.

The basic state is given by;

$$U(z) = g(\partial\theta/\partial y)(H/2-z)/(\theta f), \quad \theta(z) = -(H/2-z)\partial\theta/\partial z + 273.16$$

where;

$$\partial\theta/\partial y = -10^{-5}, \quad \partial\theta/\partial z = 39.\times10^{-4}, \quad f = 10^{-4},$$

The perturbation to this basic state, also taken from Williams (1967), coincides with the fastest growing eigen-mode, (figure 8). The specific form of the perturbation however is unimportant since the fastest growing mode would eventually dominate any finite amplitude perturbation.
The relatively short timestep of $\Lambda t = 100$ seconds was found to be necessary towards the end of the evolution when the gradients and the velocities associated with the wave were large.

Results from Experiment 2.
Some aspects of this study may be of general interest as a non-hydrostatic Eady-wave simulation; contributing to the variety of studies in the literature. We are concerned here only with those aspects relevant to the grid comparison.
The solutions from the grids were essentially identical for days 1-5 of the integration. Figures 9,10 and 11 compare the Lorenz and Charney-Phillips results at six hourly intervals between 5+1/4 days and 7 days. These results show considerably more noise in the Lorenz grid solution than in the Charney-Phillips, particularly towards the upper boundary. Figure 12 shows the u,w

and potential temperature fields at day 5+3/4, the w field shows stronger gravity wave activity on the Lorenz grid, just below the upper boundary. The increased gravity wave activity is typical of the Lorenz grid throughout the latter stages of the evolution. By day 7 the Charney-Phillips grid is also beginning to suffer from noise.

Conclusions from Experiment 2.

The primary conclusion of the Eady-wave simulation is that the solutions obtained from the two grids differ considerably in the latter stages of the evolution, and that the Lorenz grid version is noisier towards the upper boundary. This is in accordance with the results of Arakawa and Moorthi and with the expectations laid out in section 2 - supporting the suggestion that the advantages of the CP grid apply to non-hydrostatic models. It may be noted that the wave evolves more rapidly in this simulation than in that of NH. Whereas the sign of the slope of the wave reverses at about day 7, in NH this stage is not reached until day 8. It is also apparent that the meridional winds are stronger in our simulation. It is likely that the reason for these differences lies in the different form and degree of diffusion in the two models.

Note:

A result arose from this experiment which is relevant to another aspect of the new integration scheme. It was found to be necessary to update the basic state of the model regularly (every two hours) during the latter stages of the simulation. If this was not done the model became unstable. The reason for this instability lies in the fact that the explicit part of the integration scheme, which deals with the basic state, (as opposed to the perturbation quantities, which are dealt with by the implicit part), is unconditionally unstable. Hence the implicit treatment is required to keep the scheme stable at *all* courant

numbers. The effect of this is that if the model fields depart too far from the basic state the implicit treatment fails to stabilize the model, resulting in the instability experienced in this simulation. The problem of instabilities arising from the difficulty of defining suitable basic states over widely varying conditions has been recognized as a potential problem in two time-level semi-implicit *global* models. The occurrence of this instability supports the proposal in C94 to employ a semi-implicit scheme that does not subtract a global basic state in this manner.

Experiment 3. A Boundary Layer Evolution Study.

The purpose of this experiment is to investigate the performance of Charney Phillips grid based boundary layer schemes. The boundary layer scheme in the model is a so called one-and-a-half order closure scheme, (Yamada and Mellor (1979)), (the order of the closure is determined by which quantities are predicted using prognostic equations and which are paramaterized, i.e.expressed with diagnostic equations in terms of prognostic variables). The one-and-a-half order scheme has a prognostic equation for turbulent kinetic energy, (TKE), all other quantities being diagnosed. In a first order scheme *all* quantities are diagnosed. It is likely that the new integration scheme will initially use a first order scheme. At a later date a change to a one-and-a-half order scheme is possible. For this reason experiments were performed with both orders of scheme. An effective first order scheme was produced by removing the prognostic element of the TKE equation. In all matters relevant to this study the two schemes behaved similarly, hence results are only presented for the lower order scheme.

As mentioned above, the Charney-Phillips grid is less convenient for the boundary layer scheme than the Lorenz. The problem is most easily viewed as that of where to calculate the Richardson numbers, $(Ri=g*(\partial\theta/\partial z)/(\theta*(\partial u/\partial z)^2)$, (figure 13). On the Lorenz grid u,v, and θ are held at the same levels, hence the Richardson numbers naturally fall at the half levels where they are used to calculate the diffusion coefficients. On the Charney-Phillips grid however we have two alternatives; either we calculate the Ri's at the u,v levels which requires $\Delta\theta/\Delta z$ to be interpolated from adjacent layers, and subsequently interpolation of the θ diffusion coefficients, to u,v points, (the θ_bar method), or, alternatively, if we calculate the Ri's at the θ points then it is necessary to interpolate $\Delta u/\Delta z$ from adjacent layers and the momentum diffusion coefficients, to θ points, (the u_bar method).

The experiment used to investigate these options was the "Perth fog case" study of Golding (1993) (pre-frontal run), (hereafter G93). This case was studied originally as an investigation of the effect of terrain on the development of fog; it was felt to provide a demanding test of the Charney-Phillips version of the boundary layer scheme as the development is dependant on the reproduction of subtle details of the nocturnal boundary layer.

The simulation is of the development of fog at Perth (Western Australia) on the 27th of April 1990. A two dimensional domain is used with an idealized representation of the orography normal to the coast at Perth. The coast is 60km from the western boundary, with 30km of flat plain at 1m to its east, terminated by a 10km-wide scarp rising linearly to a plateau at 300m. The horizontal resolution is 5km. Experiments were performed at the vertical resolution used in the experiments of G93 (appendix 1). North-south derivatives are ignored except for the pressure gradient term in the x momentum equation. This pressure gradient remains fixed throughout the integration. Details of the synoptic situation and the surface roughness and moisture availability are as in G93. There is one significant difference between the formulation of the model used for these vertical grid experiments and that used in G93; in order to avoid unnecessary re-coding the radiation scheme was replaced in both the Charney-Phillips and the Lorenz grid versions by a simplified scheme using constant prescribed day and night-time heating rates. This only had a slight effect on the processes involved in the evolution of the boundary layer - the point of the experiment was to compare equivalent L and CP grid runs, rather than results of G93.

The simulation is initialised at 1900 local standard time, (11z). Using the modified radiation scheme described above we allow nine hours of simulated nocturnal cooling represented by a total

incoming radiation flux of 314wm^{-2}. The heating rate is then increased linearly over one hour to 1000wm^{-2} at which it is held for a further two hours as a representation of dawn and daytime heating. The following description of the relevant processes is taken from G93;

> *Winds coming off the sea are approximately westerly with 8 ms^{-1} speed. The rough land surface rapidly decelerates the near-surface air allowing the surface temperature to drop. A highly turbulent boundary layer has developed on the scarp together with a weak easterly drainage flow that locally raises wind speeds and temperatures and reduces humidity where it flows out onto the plain. These effects are diluted by surface cooling as it spreads onto the plain, but the enhanced shear generates turbulence. Between westerly winds from the sea and the easterly drainage flow, a stagnation point has formed with associated weak uplift connected to the main scarp-driven ascent. This localised reduction in horizontal wind, and the associated drop in turbulent mixing, allow saturation to occur in the lowest model layers. At the same time, the upward motion associated with the convergent wind flow assists in deepening the saturated layer.*

Results of Experiment 3.

Initially the Charney-Phillips grid version of the boundary layer scheme was written using the u_bar approach discussed above. This had a marked detrimental effect on the TKE field in both the order one and order one-and-a-half schemes; producing strong vertical oscillations and correspondingly poor distributions of potential temperature etc, (eg figure 14). To establish the sensitivities of the boundary layer scheme to interpolations of the diffusion coefficients a simple experiment was performed. The diffusion coefficients were smoothed after their calculation on the control (Lorenz) grid run by passing them through a 1-2-1 filter; this process being somewhat analogous to the interpolations required on the CP grid. The result was that

smoothing the momentum diffusion coefficients produced oscillations similar to those discussed above, (figure 15a). Performing the same filtering on the θ diffusion coefficients had virtually no impact (figure 15b). Following this result the boundary layer scheme was re-written on the CP grid using the θ_bar approach. The following results were all obtained using this method.

Figures 16-18 show the broad scale evolution of the θ, TKE and relative humidity fields at 24.0, 4.0 and 7.0 hours L.S.T. The development of the nocturnal boundary layer and its destruction by the increased turbulent mixing following sunrise can be clearly seen. On this scale there appears to be no significant difference between the results from the two grids. (Some differences exist in the relative humidity fields *above* the boundary layer, but these are likely to be due to interpolating the initial data to different levels.). Figures 19-21 compare the treatment of a number of the important features of the evolution as described above. The weak drainage flow from the scarp is handled similarly by both grids, (figure 19). At 24.00 LST the surface has been cooling for 5 hours and the drainage flow is just beginning to form, it reaches a maximum at 4.00 LST, just prior to sunrise, and is then dissipated as the surface is warmed. The area of descent is slightly greater on the CP grid than on the Lorenz at 4.00 LST. The corresponding potential temperature and relative humidity fields are shown in figures 20 and 21, respectively. The fields are similar in all cases though small differences exist in the night-time potential temperature and relative humidity fields over the low lying land. It is difficult to determine whether these differences are due to the staggering of the grids, the different heights of the model levels, or possibly a slight inconsistency in the treatment of the surface layer in the Charney-Phillips runs. (It was assumed that the CP grid surface layer was the same thickness for momentum as potential temperature. This assumption was made in the expectation that the effect would be slight, and in order to avoid altering the surface layer code).

Conclusions from Experiment 3.

The conclusion from experiment 3 is that writing the boundary layer scheme on the Charney-Phillips grid has little impact on performance, provided the temperature variables are interpolated rather than the momentum. From these tests it appears that this conclusion holds for both one and one-and-a-half order schemes.

Experiment 4. One Dimensional Boundary Layer study. (Wangara Day 33).

This experiment is a one dimensional simulation of the evolution of the boundary layer at Wangara following data taken on 16 August 1967. This data-set has been studied by a number of researchers eg. Clarke et al.(1971), Yamada and Mellor (1975) and Andrew et al.(1978). Particularly it is reported in G93 with the Perth fog case discussed above .
The approach to this experiment is the same as that of experiment 3. with a simple comparison of the Lorenz and the Charney-Phillips grid runs. It was again necessary to modify the radiation scheme; in this instance a sinusoidal solar heating rate was prescribed. i.e.

Total incoming radiation flux = $314 + 780\cos(z)$ w/m^2
where z is the zenith angle.

The integration is initialised at 0600 LST. Potential temperature, TKE and u velocity are output at 3 hourly intervals until 2400 LST. The study shows the response of the boundary layer scheme as the solar heating of the land surface produces turbulent kinetic energy and a subsequently well mixed boundary layer. The land surface then cools and the T.K.E dies away allowing a shallow inversion approximately 10 metres deep to form. At this point there is very little T.K.E above the immediate surface where a small amount is generated by wind shear.

Results from experiment 4.
Figure 22 to 24 show the control run vertical profiles of u, theta, and turbulent kinetic energy at three and six hourly intervals throughout the simulation. Despite the simplification to the radiation scheme the profiles are very similar to those in G93 and the features described above are clearly seen. Results from the Charney-Phillips grid runs are shown in Figures 25 to 27. Up to 1800 hrs both the "u_bar" and "θ_bar" versions of the Charney-Phillips grid boundary layer scheme produced

Section 4.

Conclusions and comments.

Four numerical experiments have been performed to allow direct comparison of the performance of the Charney-Phillips and the Lorenz vertical discretization schemes within a model that is very similar to that proposed as a new integration scheme for the Unified Model. The experiments examined the grids under a range of relevant flow regimes including simulations of small and large scale flows and two boundary layer studies.

Recent theoretical and experimental work with hydrostatic models has demonstrated advantages with the Charney-Phillips grid where balance aspects of the flow are important; this study indicates that these results extend to non-hydrostatic compressible models and that there is no accompanying decrease in the quality of high resolution small scale simulations.

Questions concerning the efficacy of writing the boundary layer scheme on a Charney-Phillips grid were addressed via one and two dimensional studies using both one and one-and-a-half order schemes. The results indicate that provided the interpolations necessary for writing the boundary layer scheme on the Charney - Phillips grid are performed on the temperature rather than on the momentum variables both orders of boundary layer scheme perform well.

profiles which were practically identical to the control run. After 1800 hrs the "u_bar" method retained more TKE leading to too much mixing and the failure to form an inversion. The u velocity profile is particularly poor in the u_bar results at 2100 and 2400 LST, (figures 26a,27a). The θ_bar method on the other hand reproduced the evolution of the control run faithfully.

Conclusions from Experiment 4.

This experiment reinforced the conclusions of the Perth fog case, in that the boundary layer scheme appears to work well if interpolations are carried out on the temperature variables.

Appendix 1. Heights of Model Levels for Experiment 3.

The heights of the 57 model levels of the Lorenz grid were:

1,3,5,9,16,30,50,100,150,200,250,300,350,400,450,500,550,600,

650,700,750,800,850,900,950,1000,1100,1200,1300,1400,1500,1600,

1700,1800,1900,2000,2200,2400,2600,2800,3000,3500,4000,4500,5000,

5500,6000,6500,7000,7500,8000,8500,9000,9500,10000,11000,12000.m

References.

Andrew,J.C.,De Moor,G.,Lacarrere,P.,Therry,G.and Du Vachat,R.1978: Modelling the 24 hour evolution of the mean and turbulent structures of the planetary boundary layer. J.Atmos.Sci.,35,1861-1883.

Andrews,P.L.,1993:An extra balance step for the UK Met.Office's assimilation code.,Research Activities in Atmospheric and Oceanic Modelling Report No. 18.

Arakawa,A.,1962:Non-geostrophic effects in the baroclinic prognostic equations.Proceedings International Symposium Numerical Weather Prediction.WMO,Tokyo,161-175

_____,1983:Vertical differencing of the primitive equations.,Proc.ECMWF Seminar on numerical methods for Weather prediction.,Vol.1,207,224.

_____**and Suarez,M.**,1983:Vertical differencing of the primitive equations in sigma coordinates. Mon.Weather Rev.,11,34-45.

_____**and Moorthi,S.**,1987:Baroclinic instability in vertically discrete systems.J.Atmos.Sci.,Vol.45,No.11, 1688-1707.

Carpenter, R.L., Droegemeier, K.K., Woodward, P.R. and Hane,C.E. 1990:Application of the piecewise parabolic method (PPM) to meteorological modelling.,Mon.Weather.Rev.,118,586-612.

Charney,J.G. and Phillips,N.A.,1953:Numerical integration of the quasi-geostrophic equations for barotropic and simple baroclinic flows.J.Meteor.,10,71-99.

Clarke,P.D. and Haynes,P.H.,1993:Equatorial inertial instability: effects of vertical finite differencing and radiative transfer. J.Atmos.Sci.,51,No.14,2101-2109.

Clarke,R.H.,Dyer,A.J.,Brook,R.T.,Reid,D.G. and Troup,A.J.1971: The Wangara experiment-Boundary layer data.Paper No.19,Division of Meteorological Physics,CSIRO,Australia,362pp.

Cullen,M.J.P.,Davies,T. and Mawson,M.H.1994:A semi-implicit integration scheme for the Unified Model. F.R.Working Paper No. 154 (Version no.6)

Fox-Rabinovitz,M.S.,1993:Computational dispersion properties of vertically staggered grids for atmospheric models. Mon.Weather Rev.,122,377-392.

Golding,B.W.,1992:An efficient non-hydrostatic forecast model. Meteor.Atmos.Phys.,50,89-103.

__ 1993:A study of the influence of terrain on fog development. Mon. Weather Rev, 121,2529-2541.

Leslie,L.M. and Purser,R.J.,1992:A comparative study of the performance of various vertical discretization schemes. Meteorol.Atmos.Phys.50,61-73.

Lorenz,E.N.,1960:Energy and numerical weather prediction. Tellus,12,364-373.

Nakamura,N. and Held,I.M.,1989:Nonlinear equilibration of two-dimensional Eady waves. J.Atmos.Sci.,46,No.19,3055-3064.

_____.1994:Nonlinear equilibration of two dimensional Eady waves: simulations with viscous geostrophic momentum equations.,J.Atmos.Sci.,51,No.7.,1023,1035.

Orlanski,I.,1986:Localized baroclinicity: A source for meso-α cyclones.J.Atmos>Sci.,43,2857-2885.

Simmons, A.J. and Hoskins,B.J.,1967:The life cycles of some non-linear baroclinic waves.J.Atmos.Sci.,34,1619-1633.

Schneider,E.K.,1987:An inconsistency in vertical discretization in some atmospheric models. Mon.Weather Rev.,115,2166-2169.

Williams,R.T.,1967:Atmospheric frontogenesis: A numerical experiment. J.Atmos.Sci.,29,3-10.

Yamada,T. and Mellor,G.L.,1975:A simulation of the Wangara atmospheric boundary layer data.J.Atmos.Sci.,32,2309-2329.

_____1979:A numerical simulation of BOMEX data using a turbulence closure model coupled with ensemble cloud relations. Quat.J.Royal Met.Soc.,105,915.

Globally Averaged Percentage Error in Geopotential.

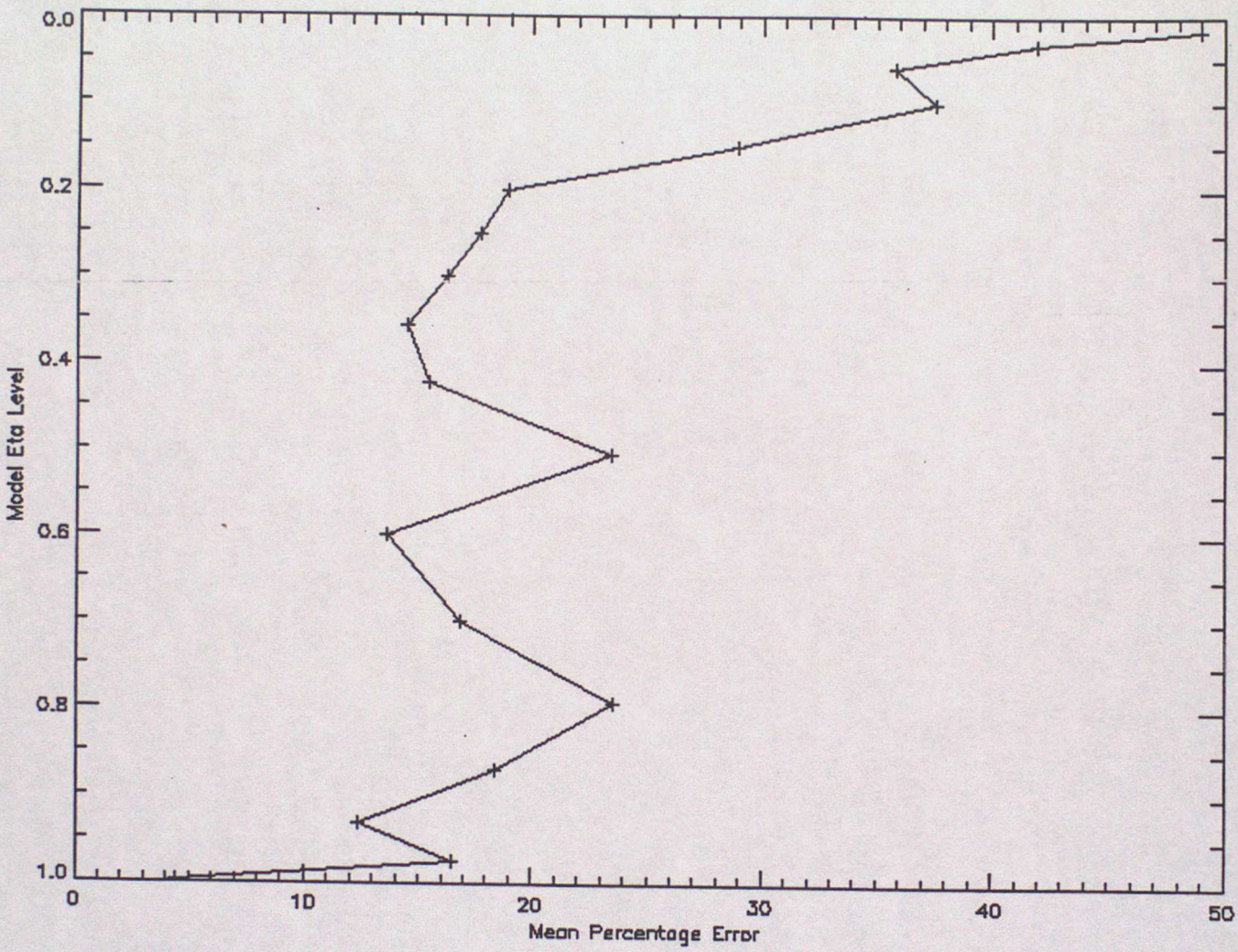

Fig.1. Comparison of retransformed geopotential increment field with wind derived geopotential increment field. The original geopotential field is derived from non surface wind observations. The percentage error is determined by dividing the rms difference between the two fields by the rms value of the original field, and multiplying by 100%. Note that a model eta level of 1 corresponds to the surface, and of 0 to outer space.

The Charney-Philips and the Lorenz vertical grids.

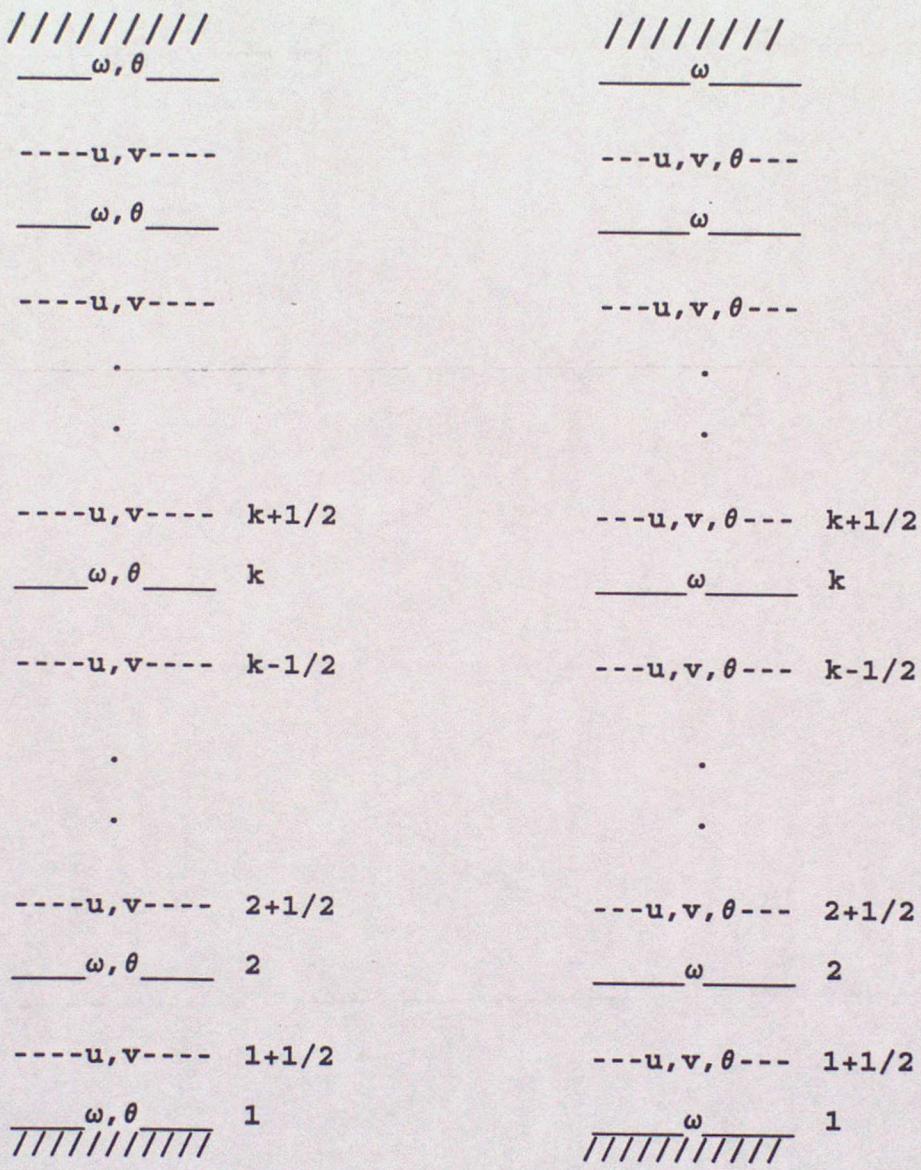

Fig.2. The Charney-Philips grid (1953) and the Lorenz grid (1960).

Relative positions of the Potential temperature levels on the Charney-Philips and the Lorenz grids.

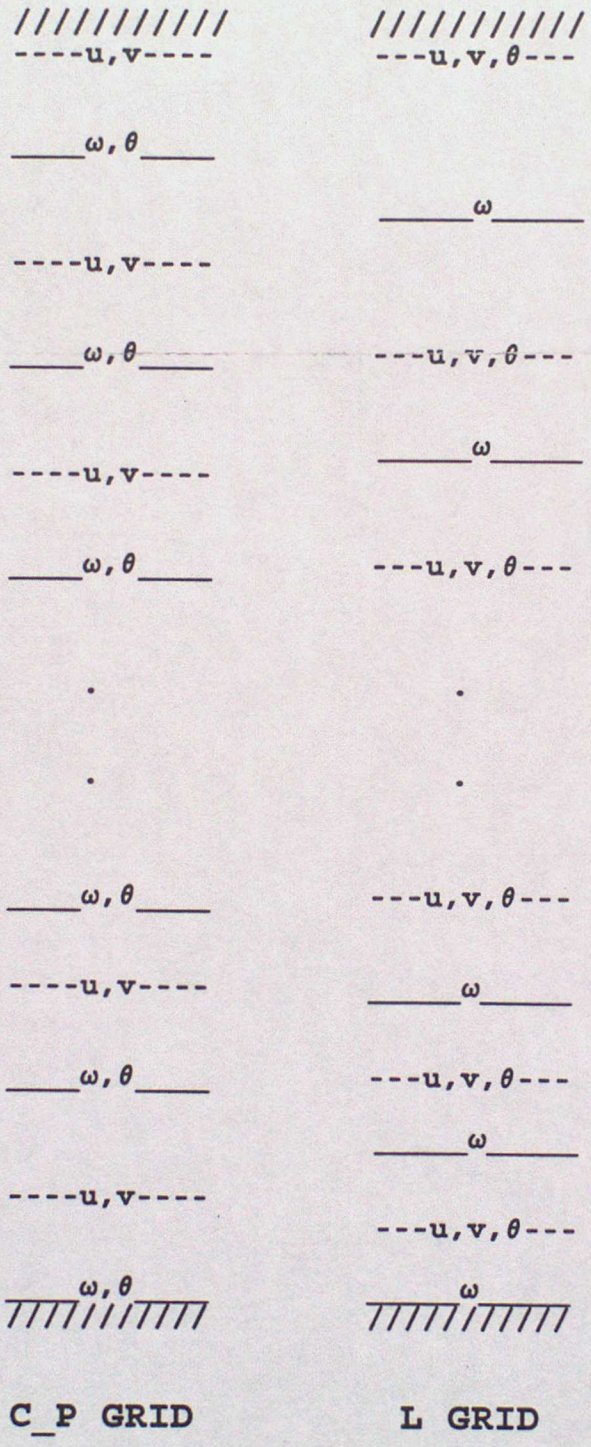

Fig.3. Heights of the potential temperature levels for the cold gravity current experiment.

Evolution of the Cold Gravity Current

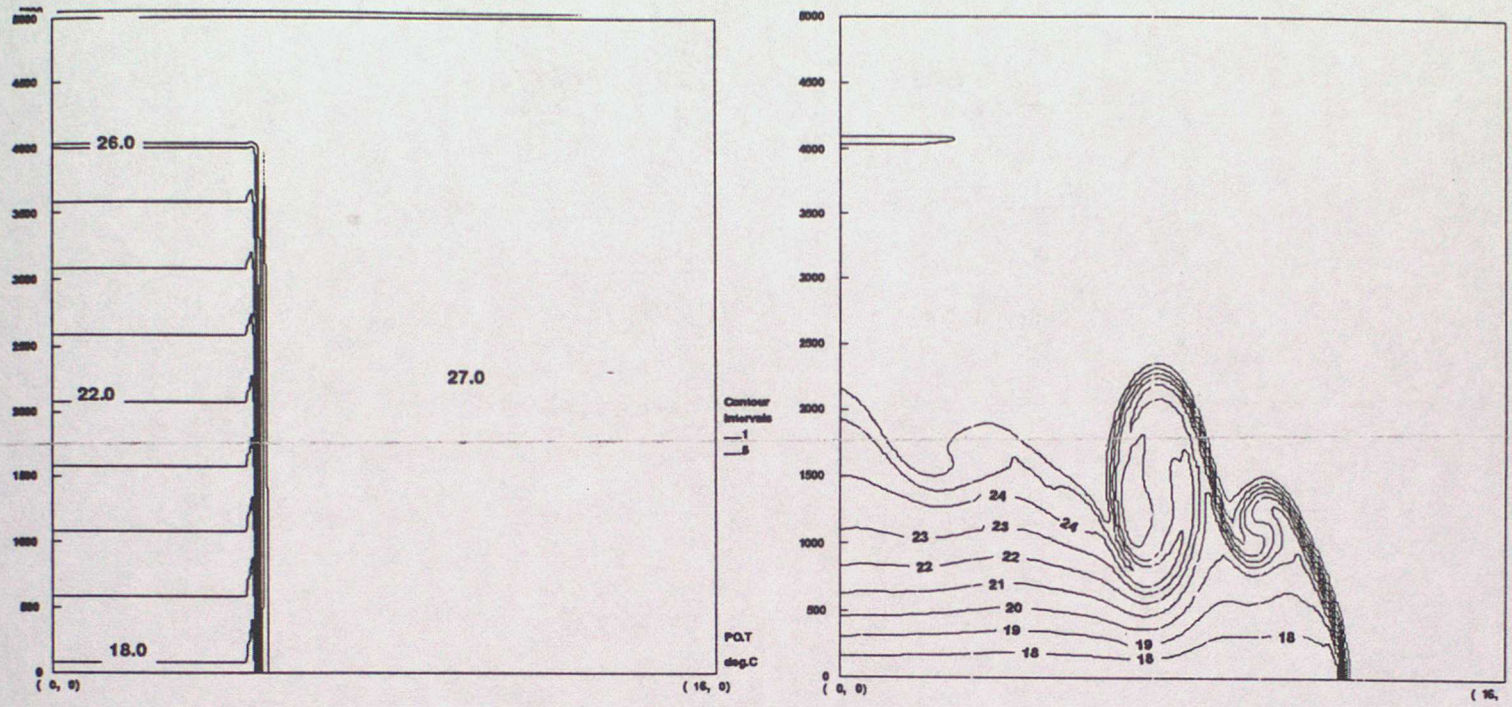

a) t = 0.

b) t = 500s

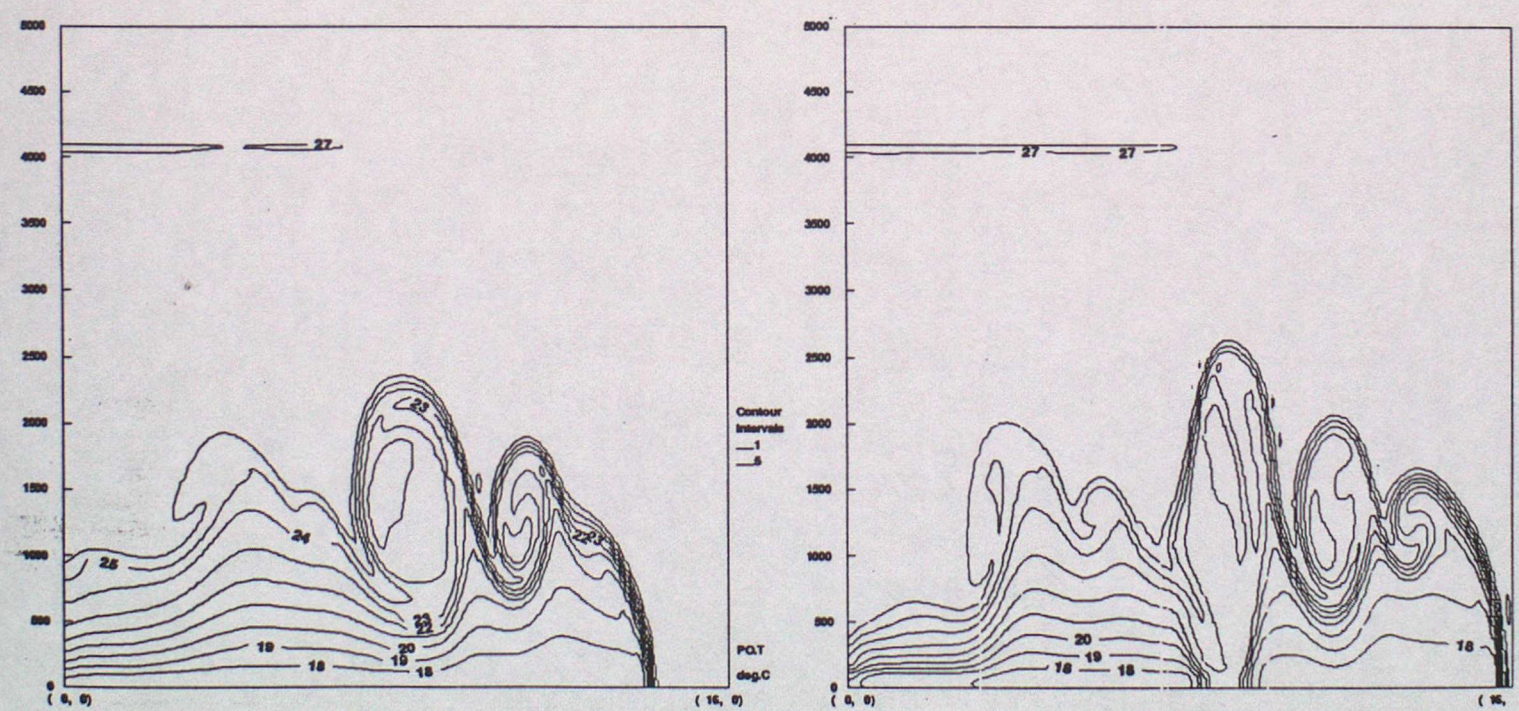

c) t = 600s

d) t = 750s

Fig.4. The first 750 seconds of the cold gravity current.

Cold Gravity Current on the CP and L Grids.

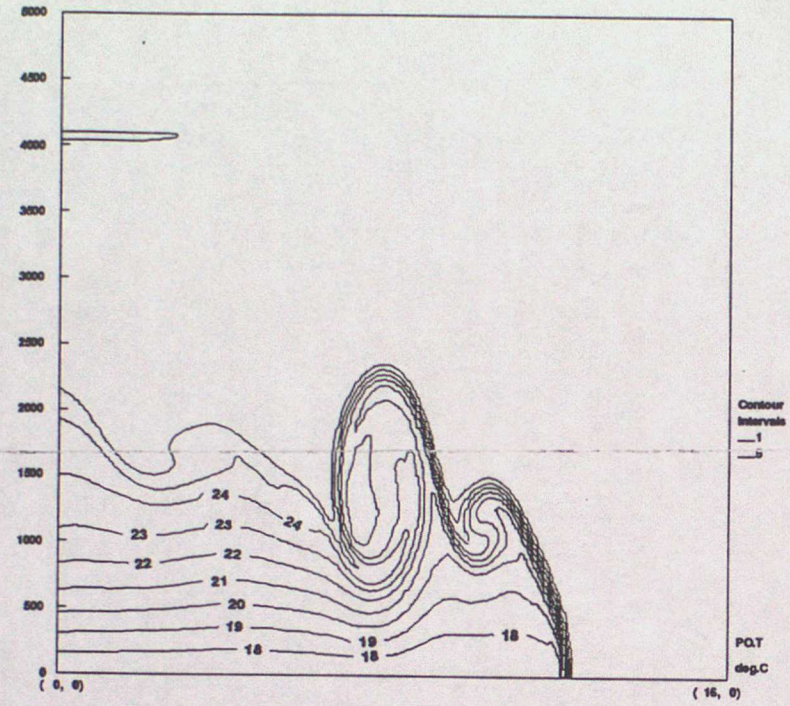

a) L Grid, Δz=83m

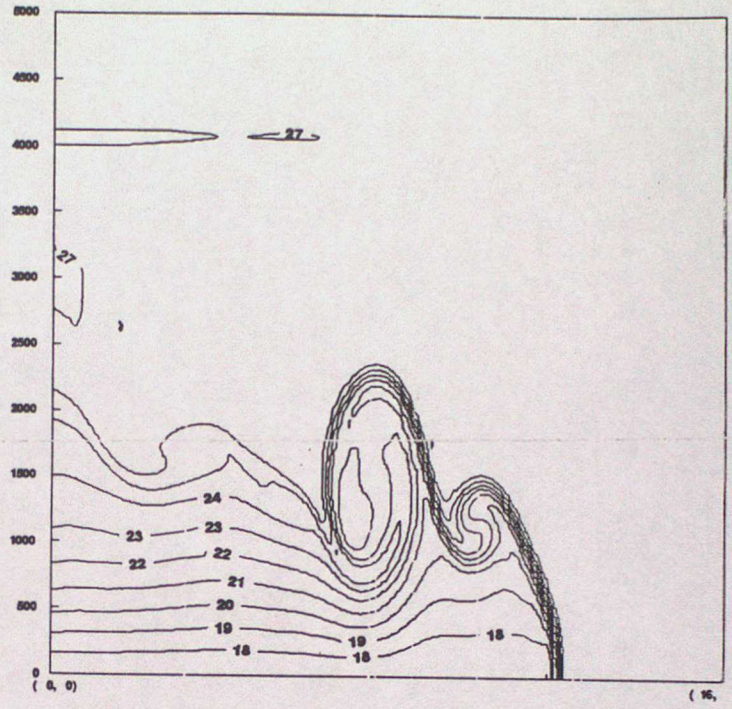

b) CP grid, Δz=83m

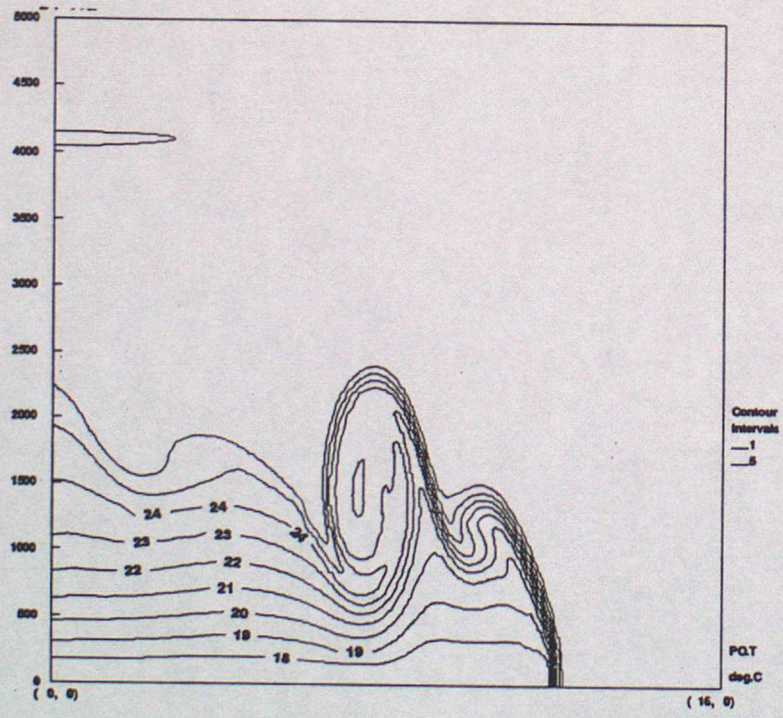

c) L Grid, Δz=125m

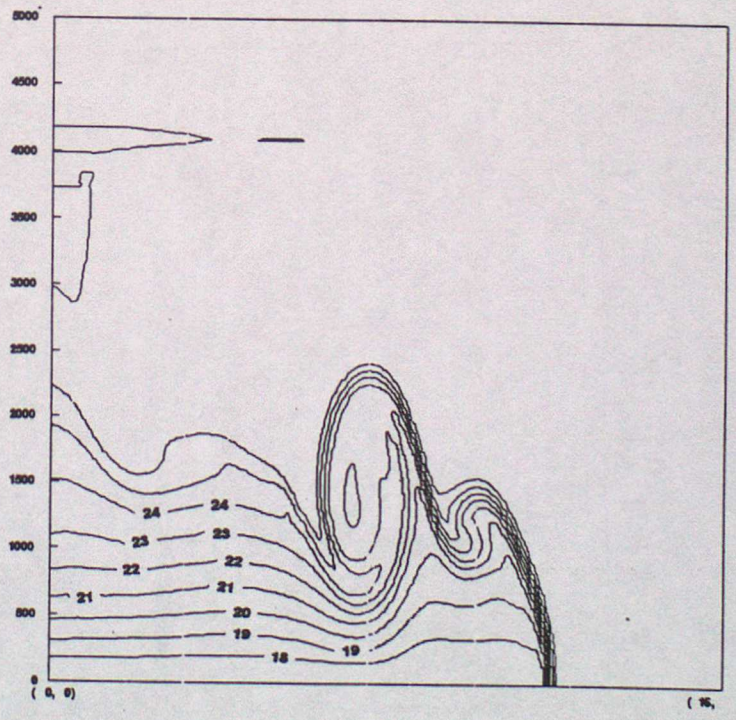

d) CP Grid, Δz=125m

Fig.5. CP and L grid solutions at coaser vertical resolutions.(Δt = 500s).

Cold Gravity Current on the CP and L Grids.

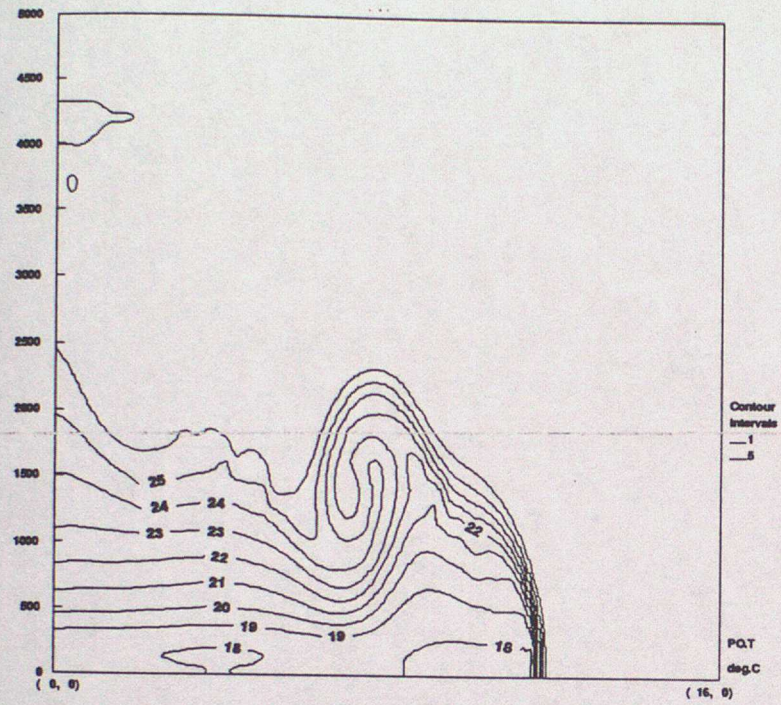

a) L Grid, Δz=250m

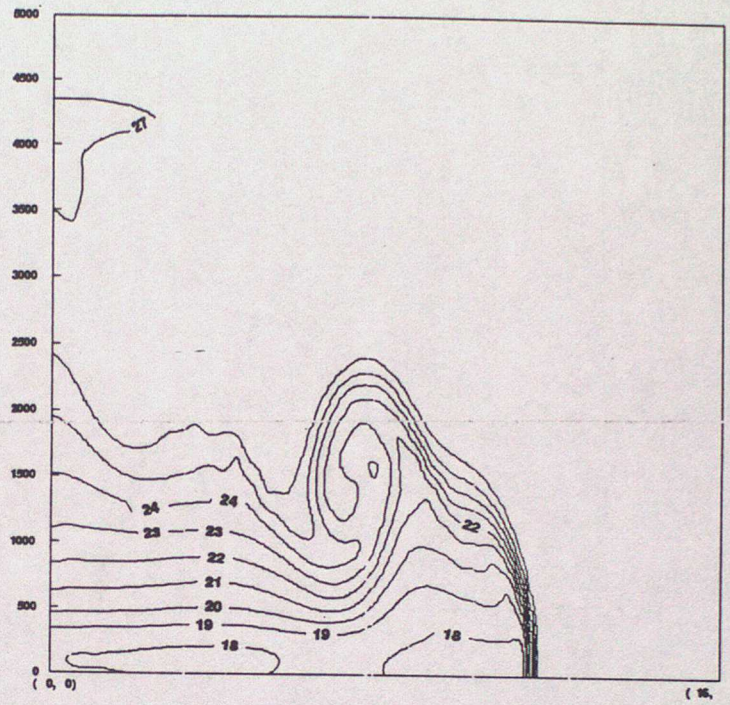

b) CP grid, Δz=250m

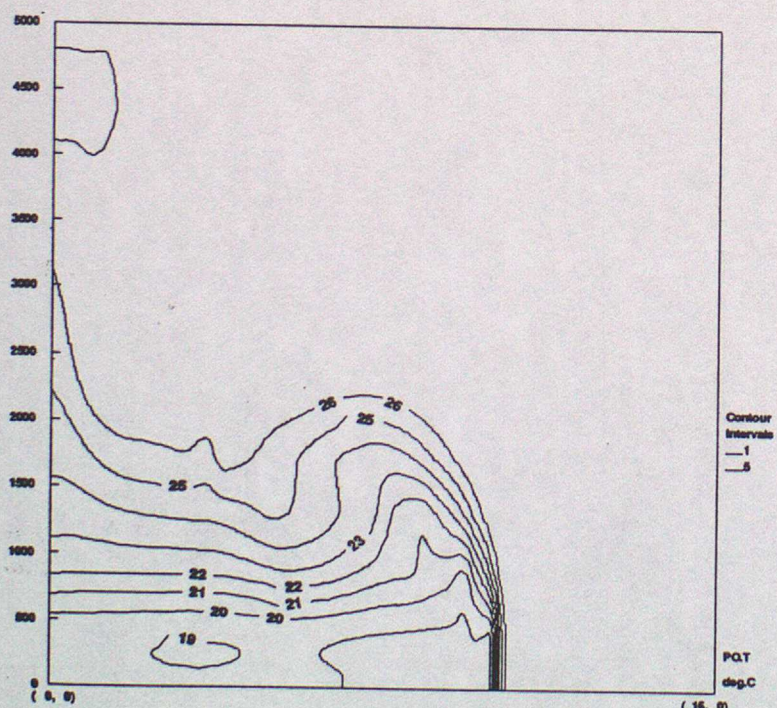

c) L Grid, Δz=500m

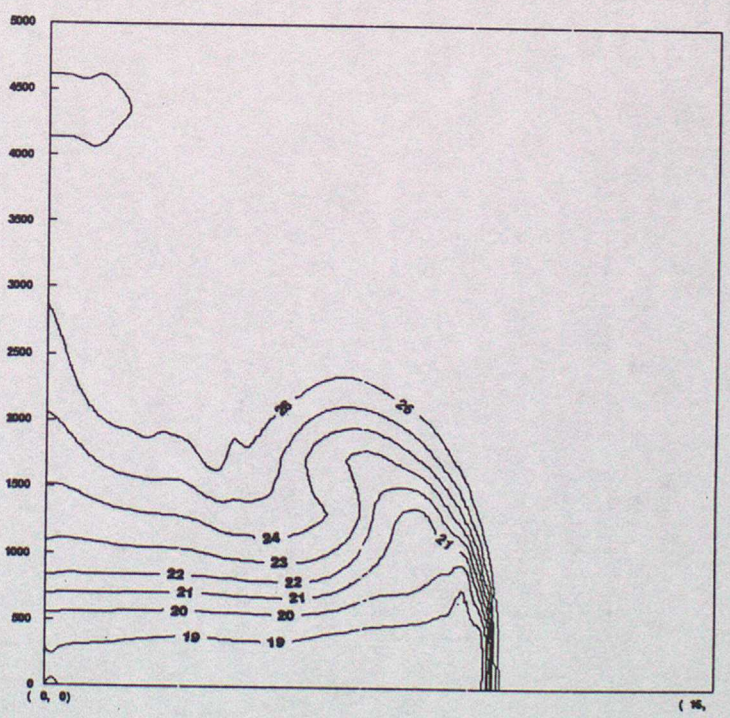

d) CP Grid, Δz=500m

Fig.6. CP and L grid solutions at coaser vertical resolutions. (Δt = 500s).

Results From Nakamura and Held (1989).

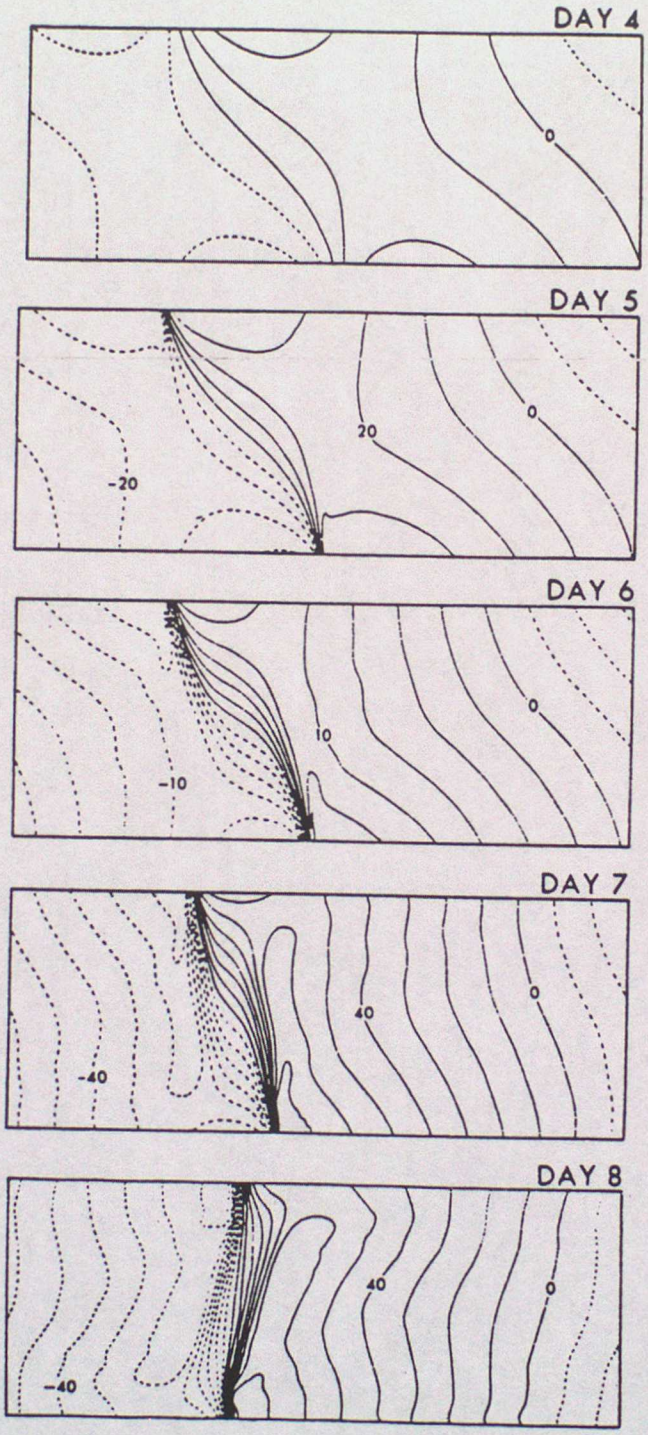

FIG. 2. Evolution of x–z structure of v-field for the control run. λ = 2000 km, Ri = 25. Contour interval is 10 m s^{-1}.

Fig.7. Evolution of x-z structure of v-field. From Nakamura and Held (1989).

Perturbation to the Basic State

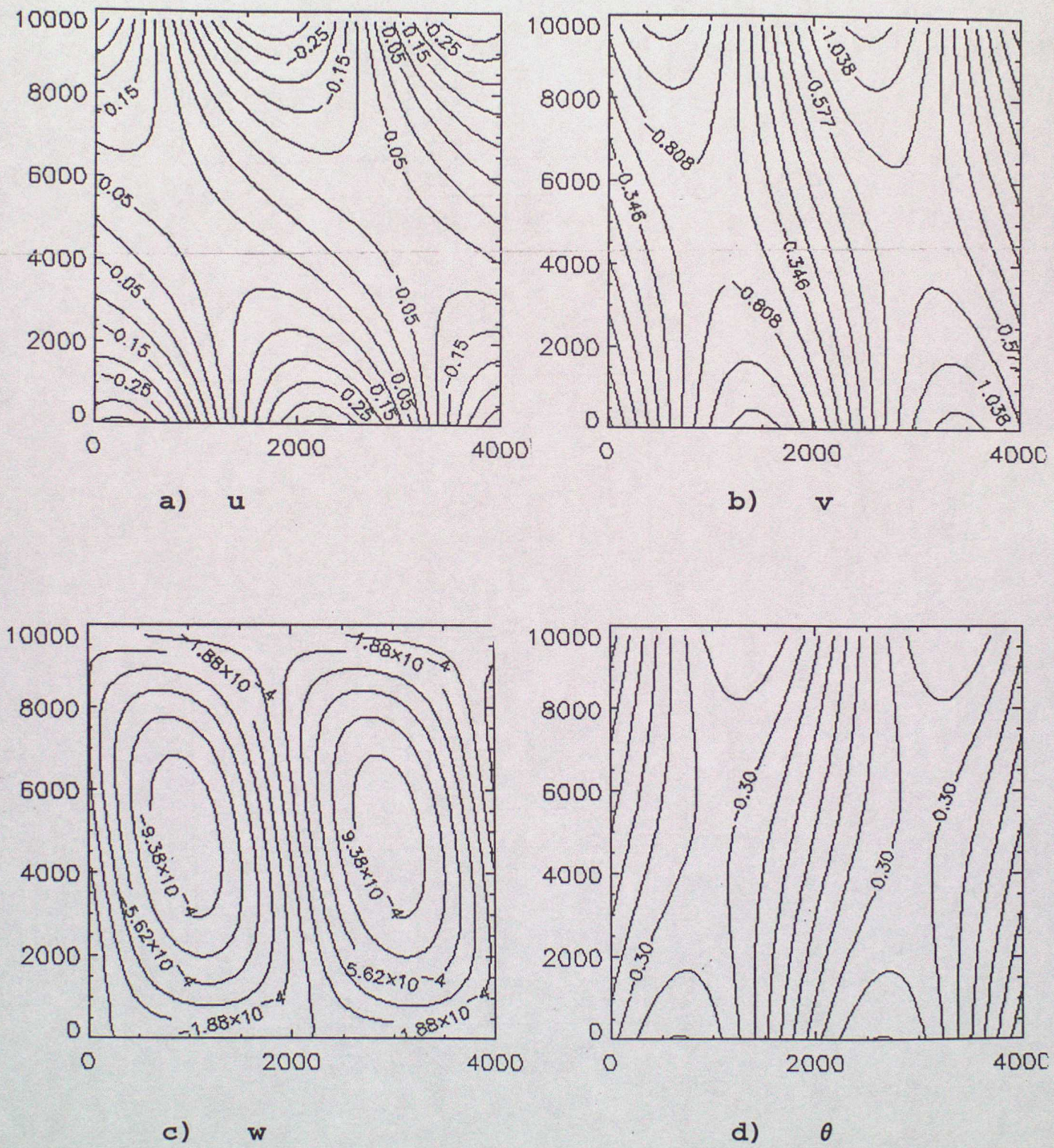

Fig.8. The perturbation to the basic state corresponding to the fastest growing eigen mode. (Williams 1967).

Eady waves on the CP and L grids.

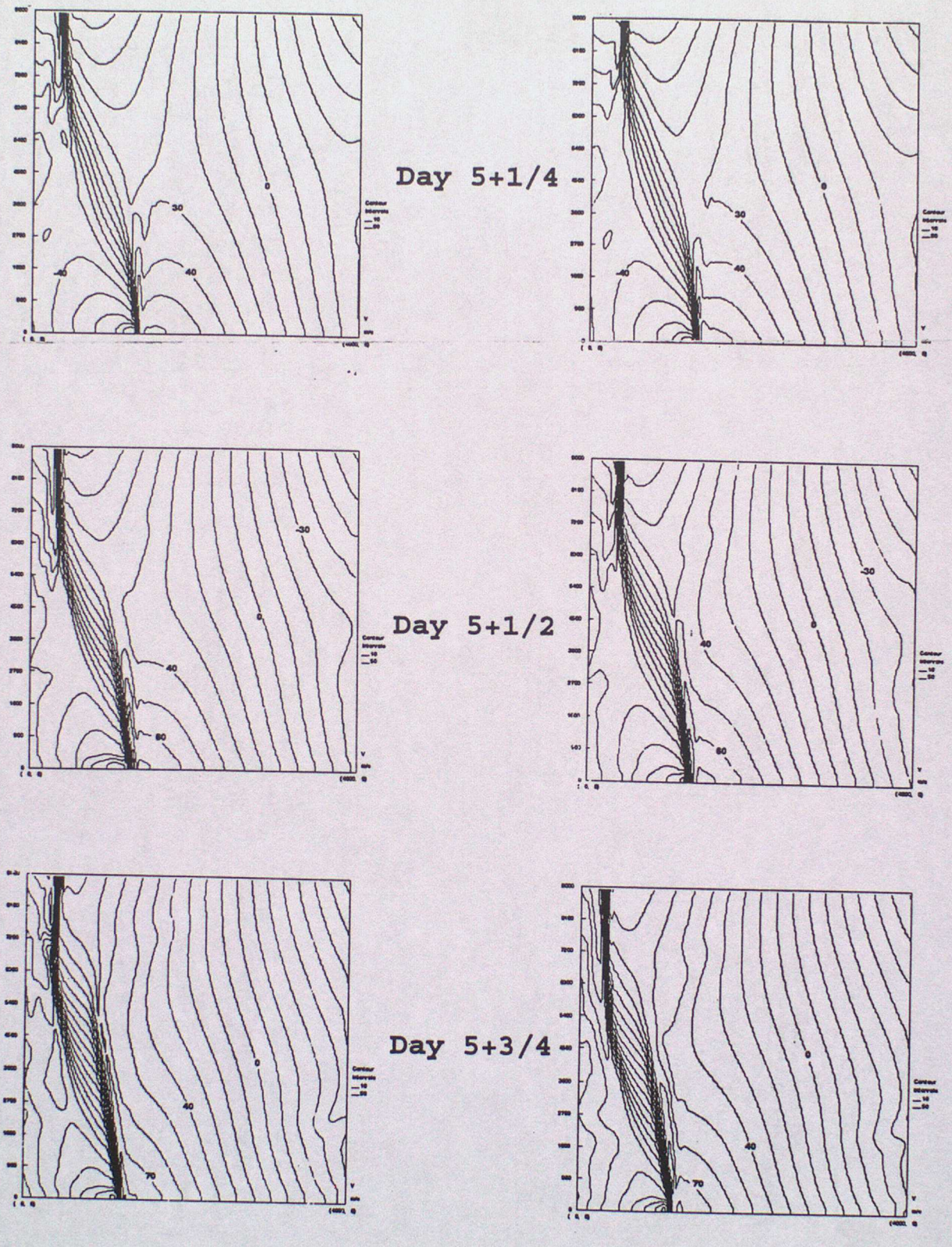

Fig.9. v component of velocity for the CP and L grids. (contour interval is $10ms^{-1}$)

Eady waves on the CP and L grids.

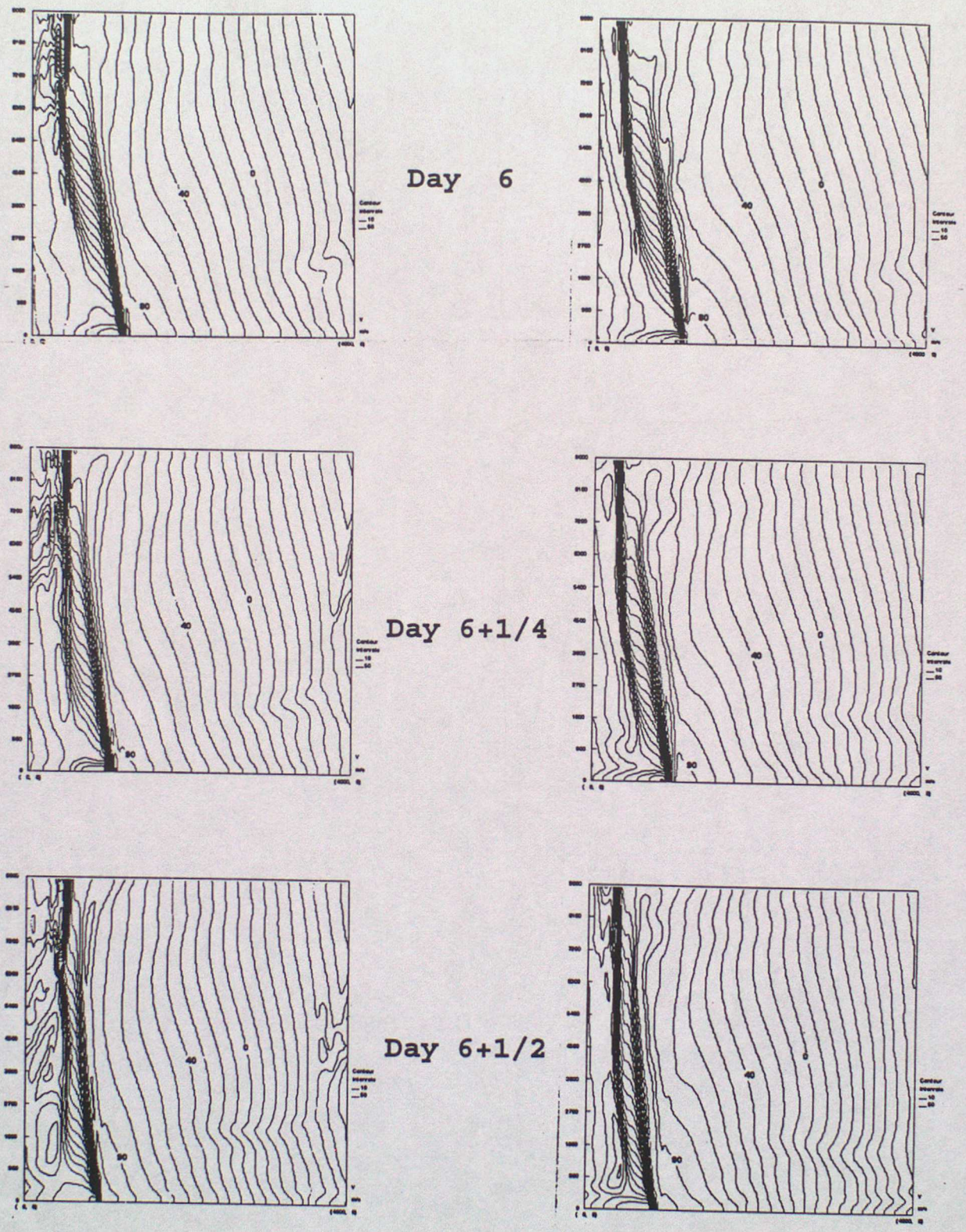

Fig.10. v component of velocity for the CP and L grids. (contour interval is $10ms^{-1}$)

Eady waves on the CP and L grids.

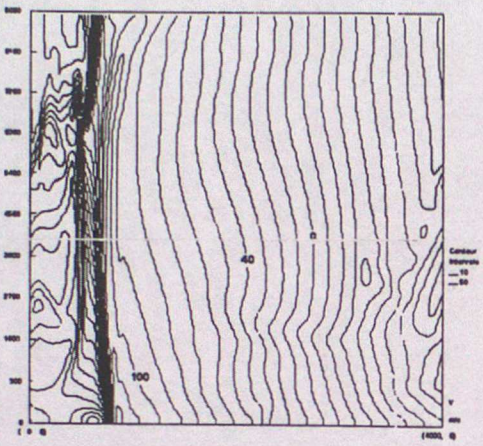

Day 6+3/4

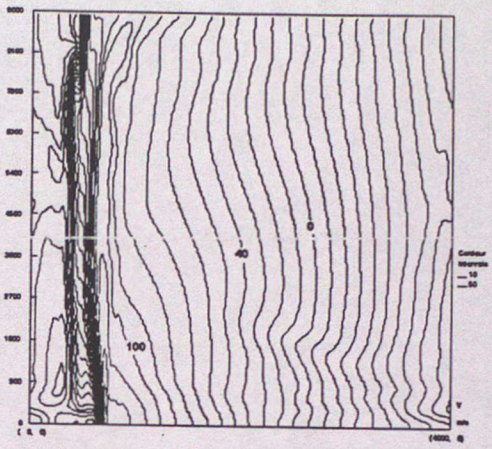

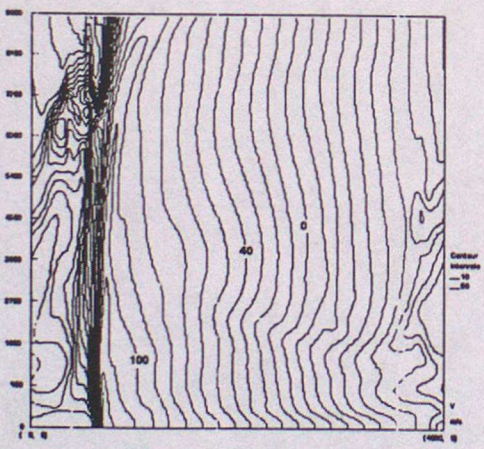

Day 7

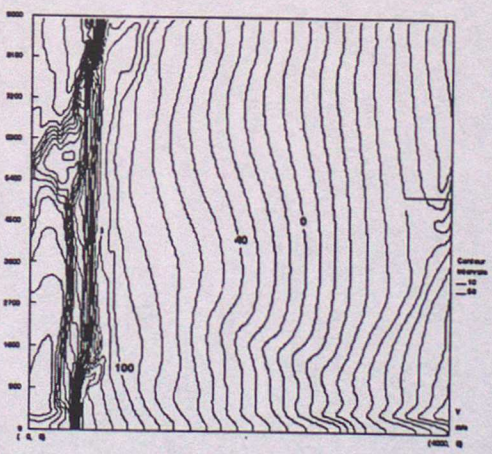

L Grid.

CP Grid.

Fig.11. v component of velocity for the CP and L grids. (contour interval is $10ms^{-1}$)

Eady waves on the CP and L grids.

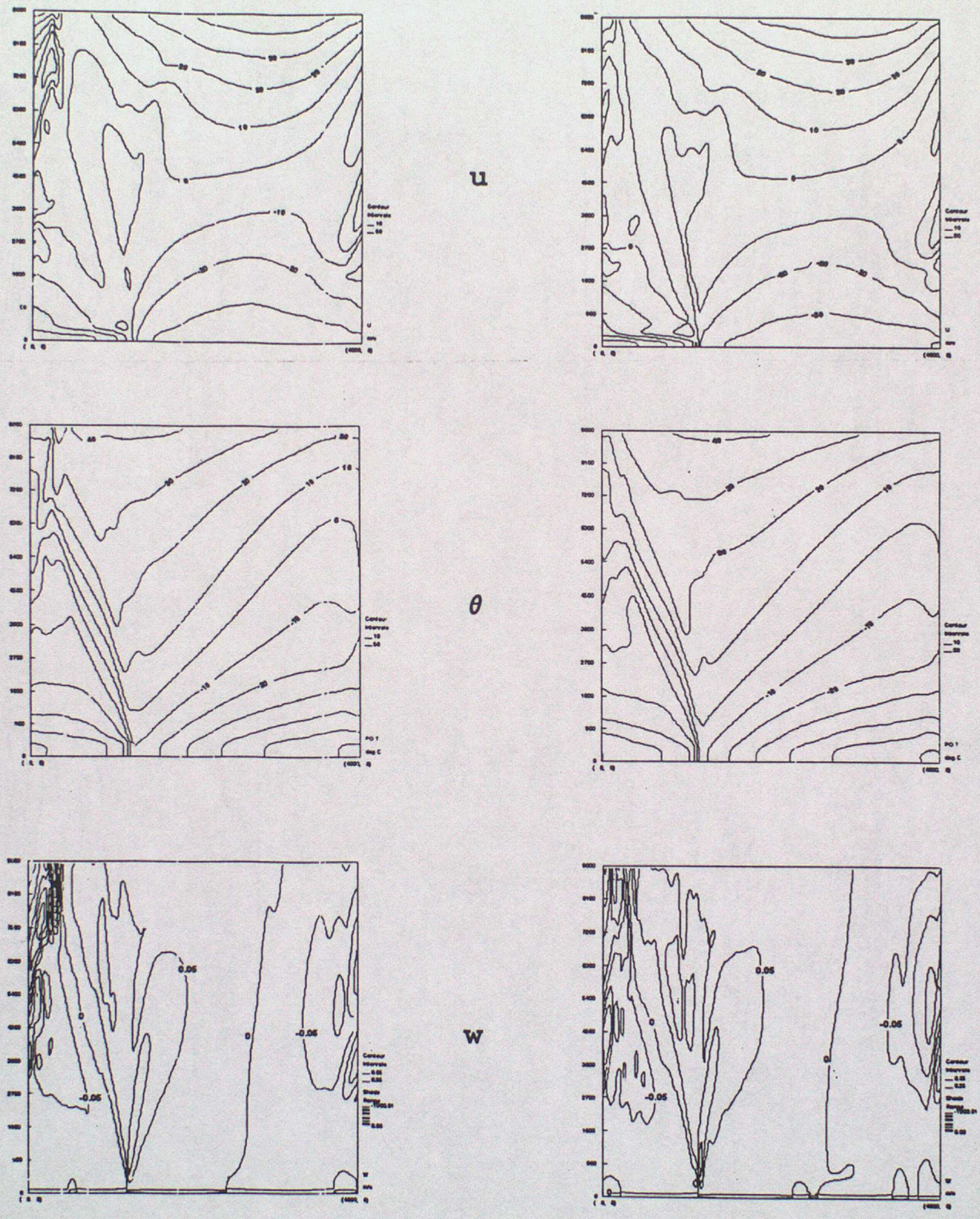

Fig.12. The u,v and w fields at 5+3/4 days showing increased gravity wave activity and noise near the upper boundary on the L grid.

Boundary layer scheme on the Lorenz grid

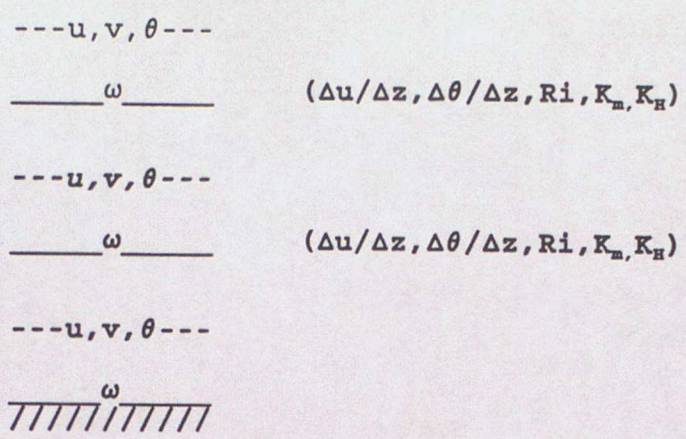

Boundary layer scheme on the Charney-Phillips grid.

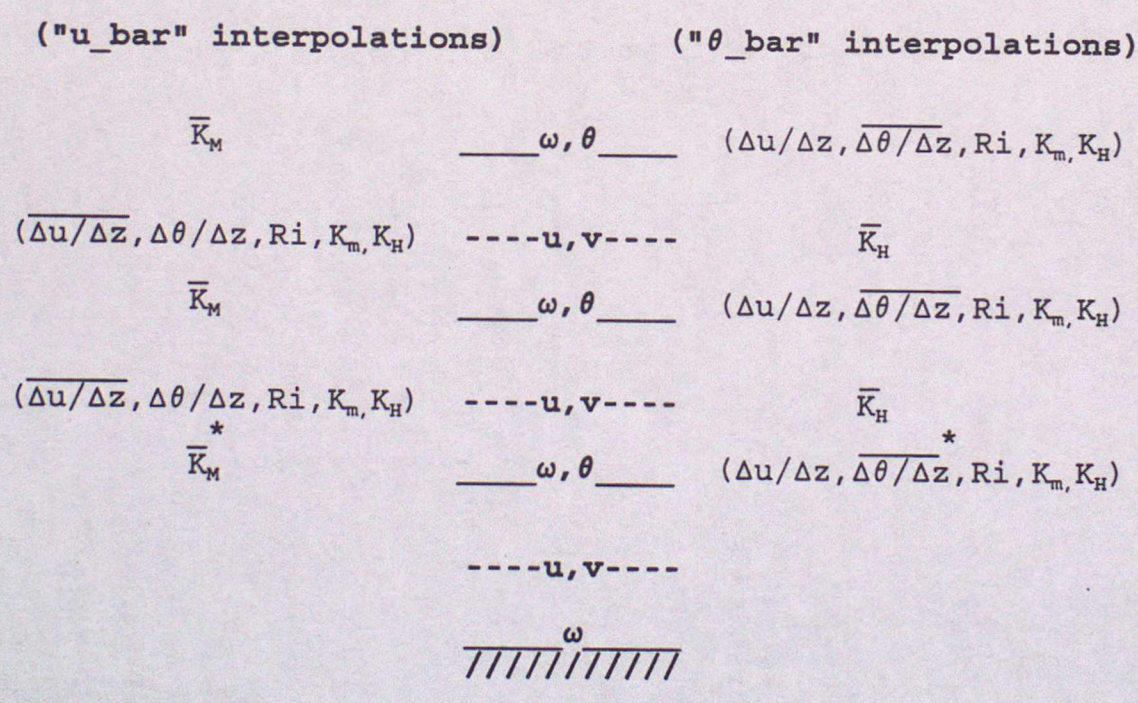

Fig.13. Options for the boundary layer scheme on the Charney-Philips grid. (An overbar indicates an interpolated quantity and a star indicates a one-sided interpolation)

TKE and Potential Temperature using "uv_Bar" method.

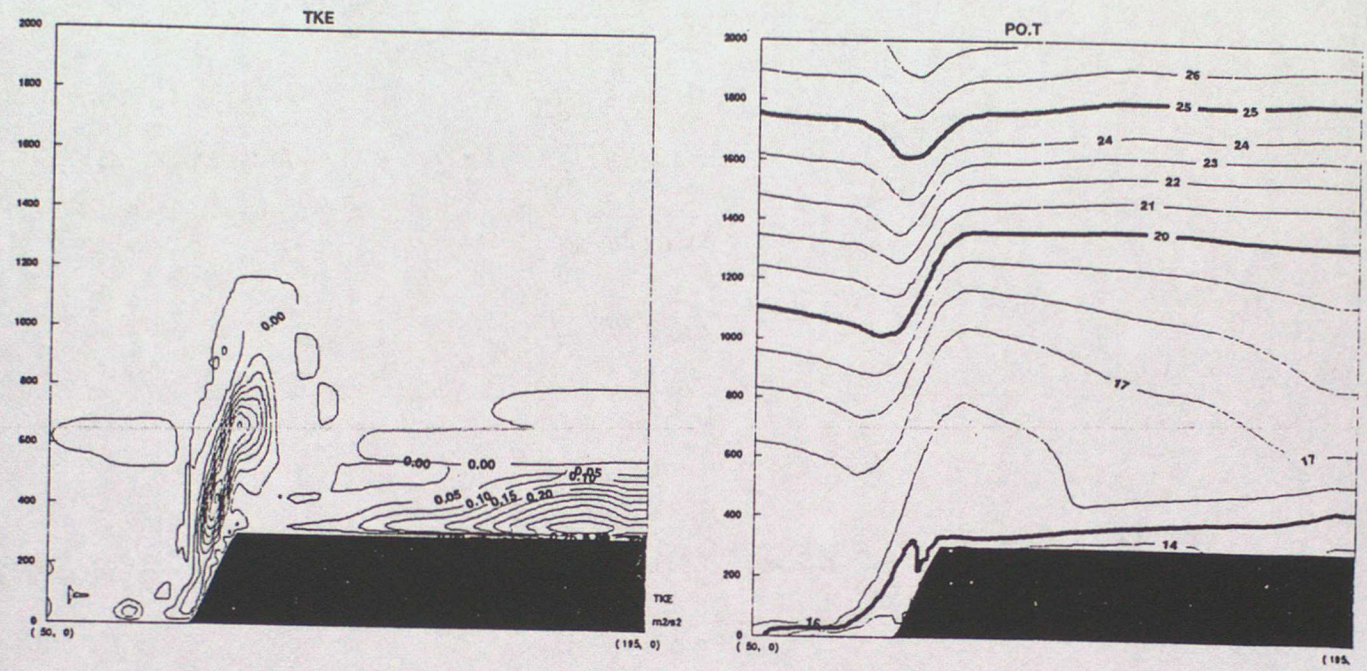

a) TKE and θ from the control run at 20z.

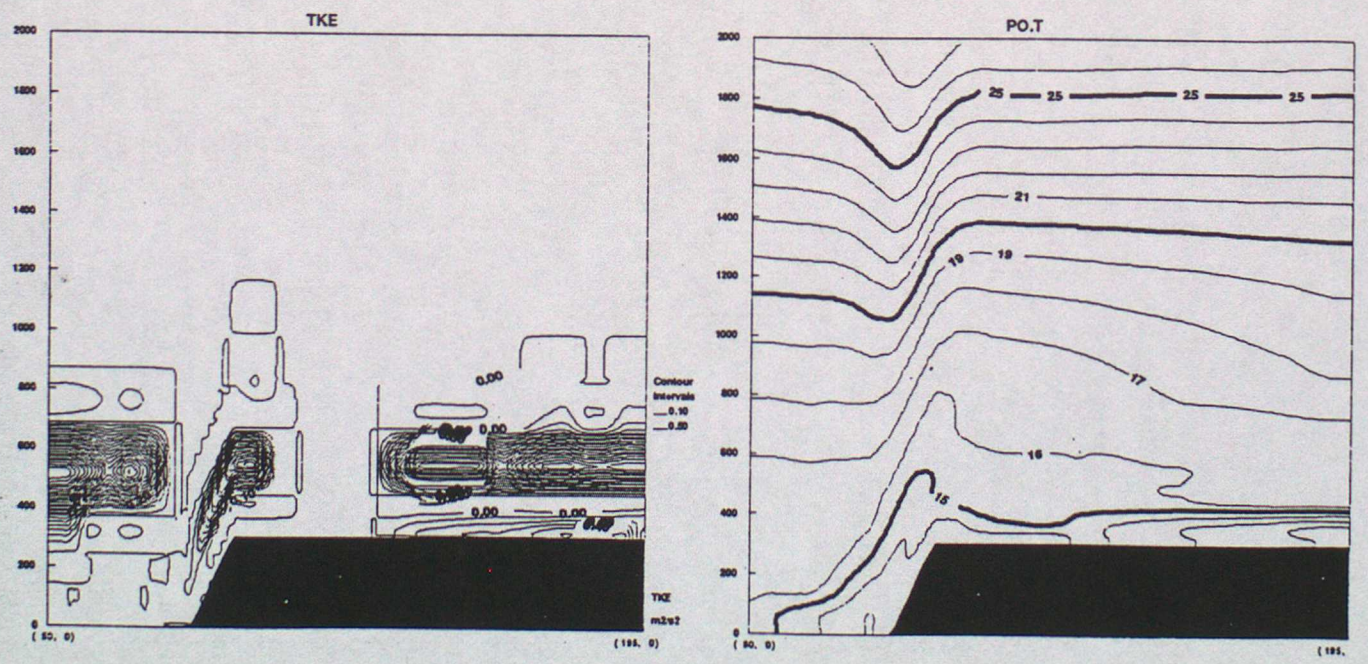

b) TKE and θ from the CP run (uv_bar) at 20z.

Fig.14. Oscillations in TKE field following the interpolations in u,v and the momentum diffusion coefficients required by the uv_bar approach.

TKE and Potential Temperature after smoothing Diffusion Coefficients.

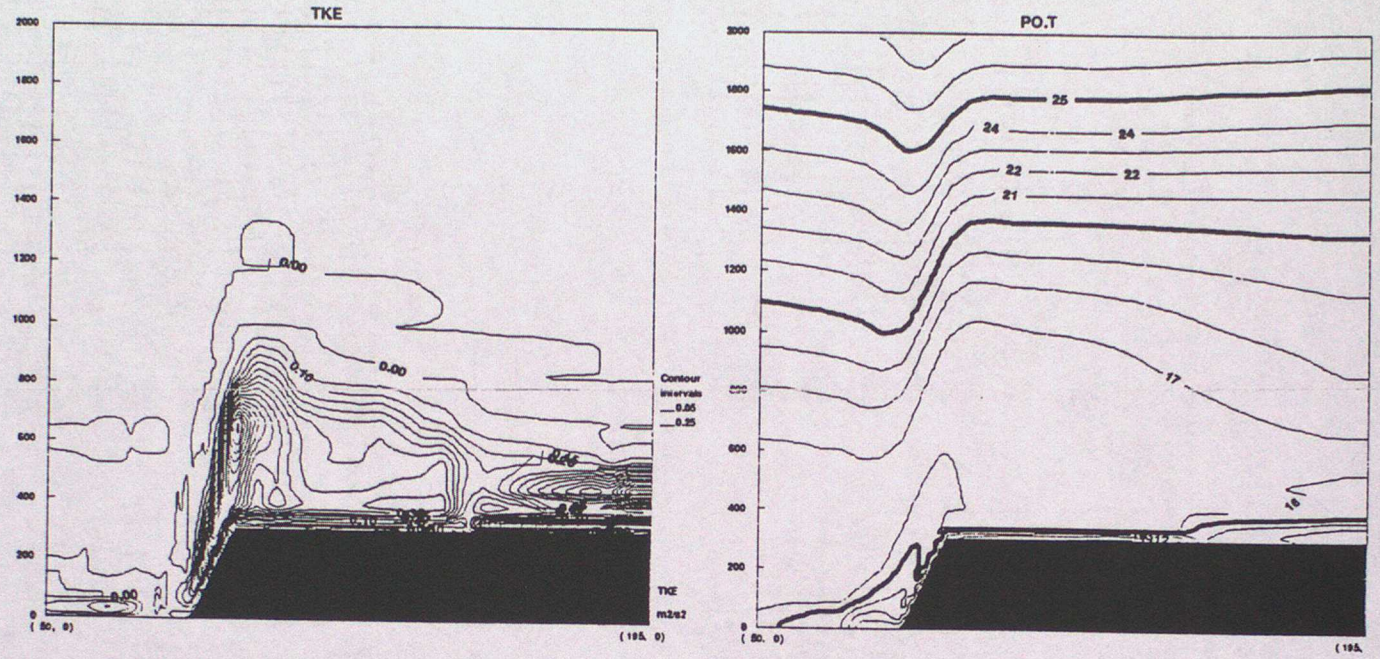

a) u,v diffusion coeffs. smoothed.

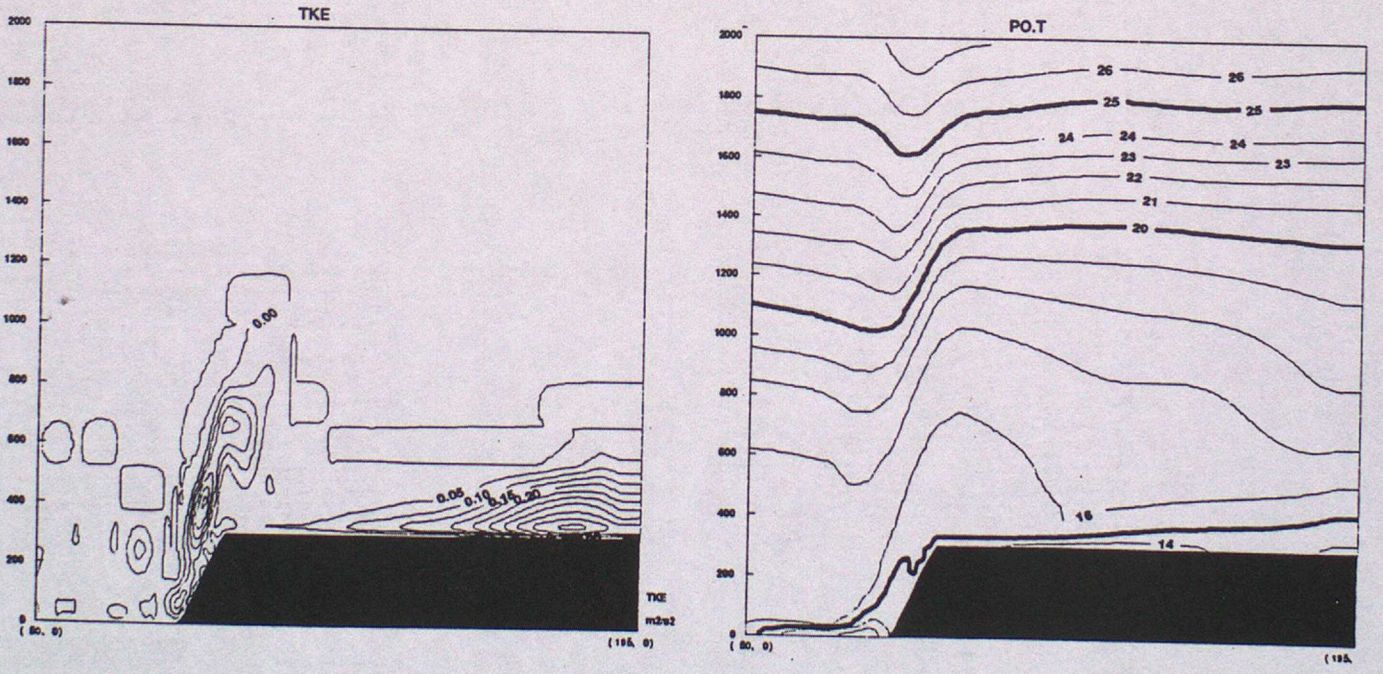

b) θ diffusion coeffs. smoothed.

Fig.15. The effect of smoothing the momentum and potential temperature diffusion coefficients. (for control run see figure 14a

Broad Scale evolution of Potential Temp.

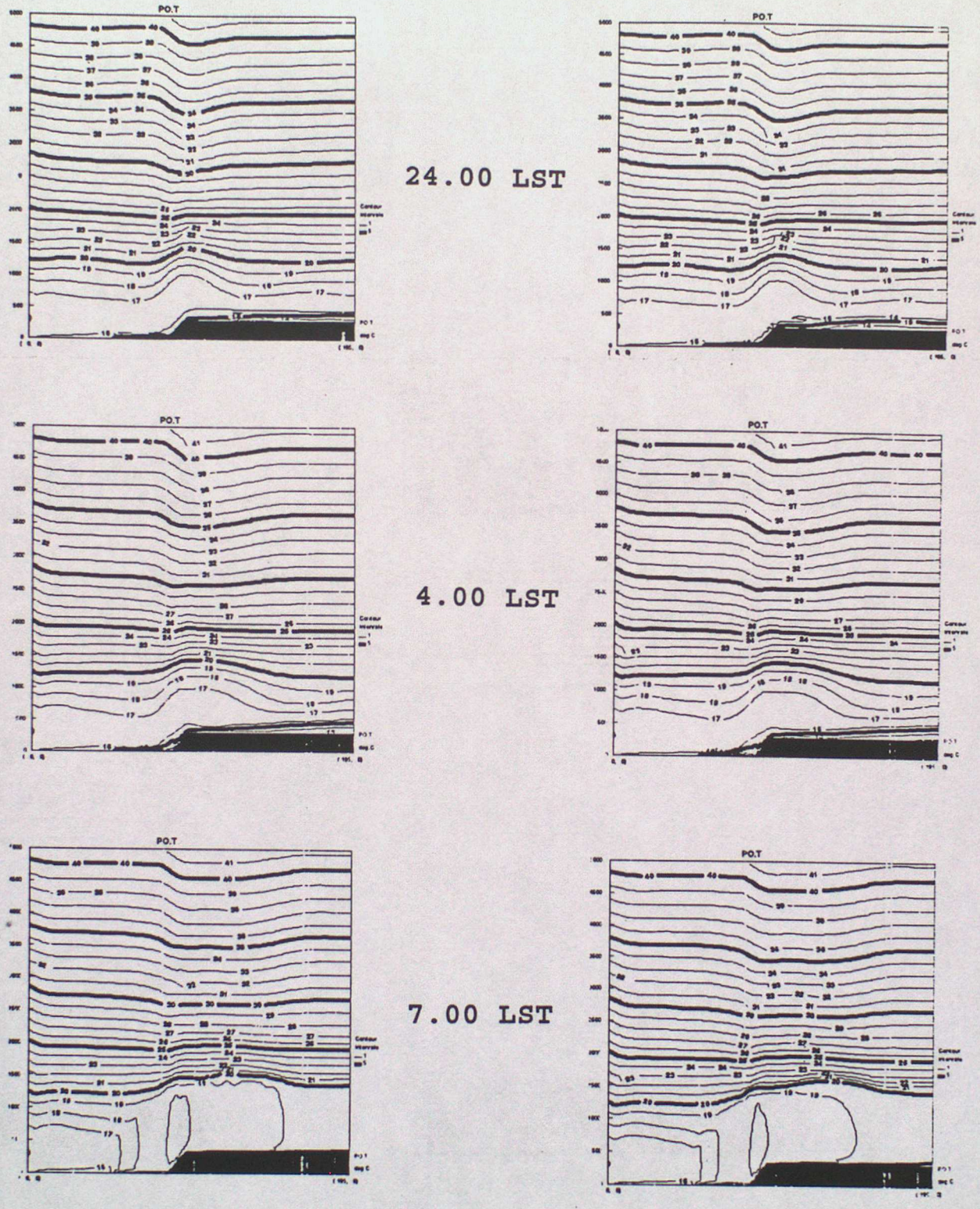

Fig.16. Broad scale evolution of θ at 24.0 LST (4 hours before sunrise), 4.0 LST (immedeately prior to sunrise) and 7.0 LST (after sunrise plus 2 hours daytime heating).

Broad Scale evolution of T.K.E.

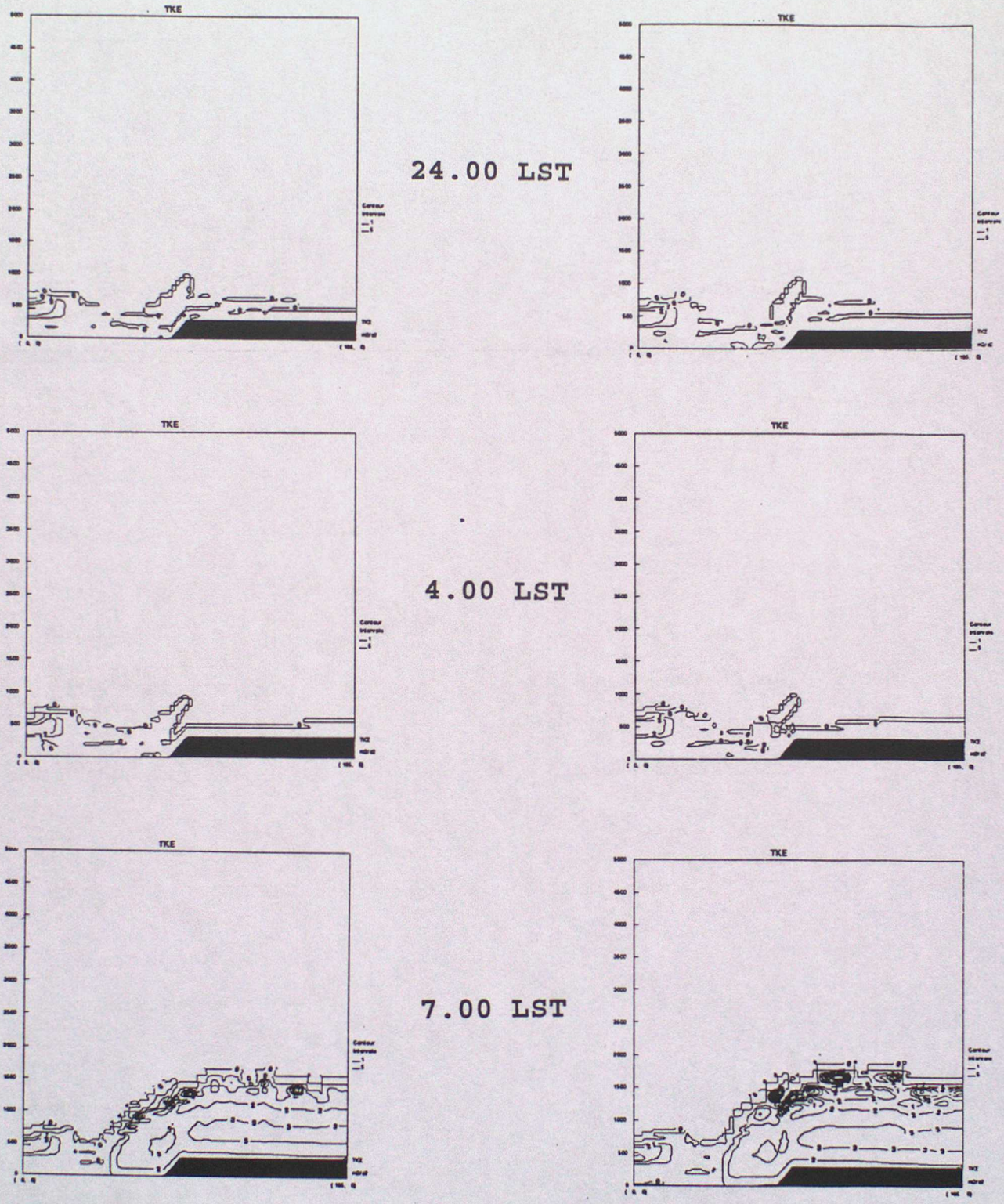

Fig.17. Broad scale evolution of TKE at 24.0 LST (4 hours before sunrise), 4.0 LST (immedeately prior to sunrise) and 7.0 LST (after sunrise plus 2 hours daytime heating).

Broad Scale evolution of Relative Humidity.

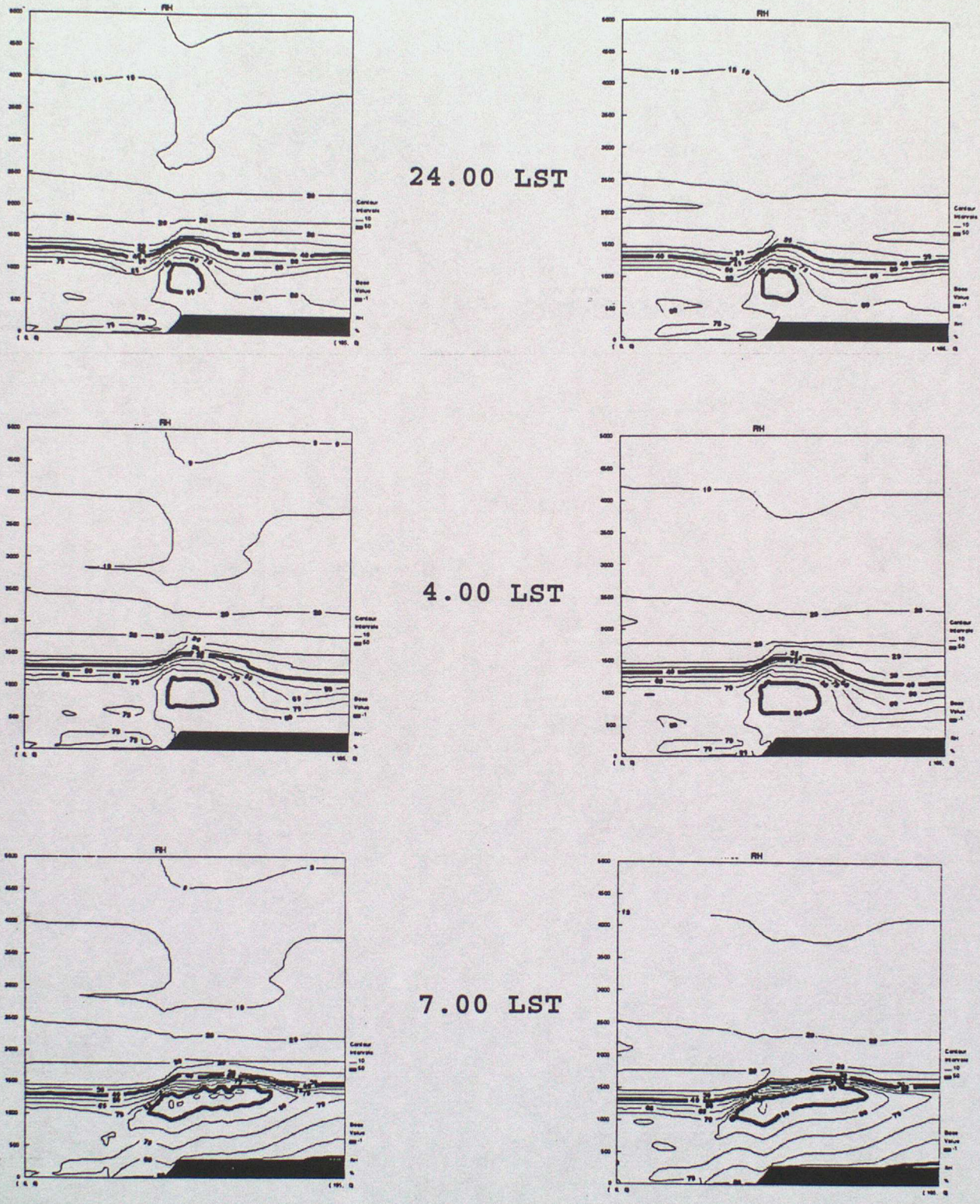

Fig.18. Broad scale evolution of RH at 24.0 LST (4 hours before sunrise), 4.0 LST (immedeately prior to sunrise) and 7.0 LST (after sunrise plus 2 hours daytime heating).

Evolution of the Drainage Flow.

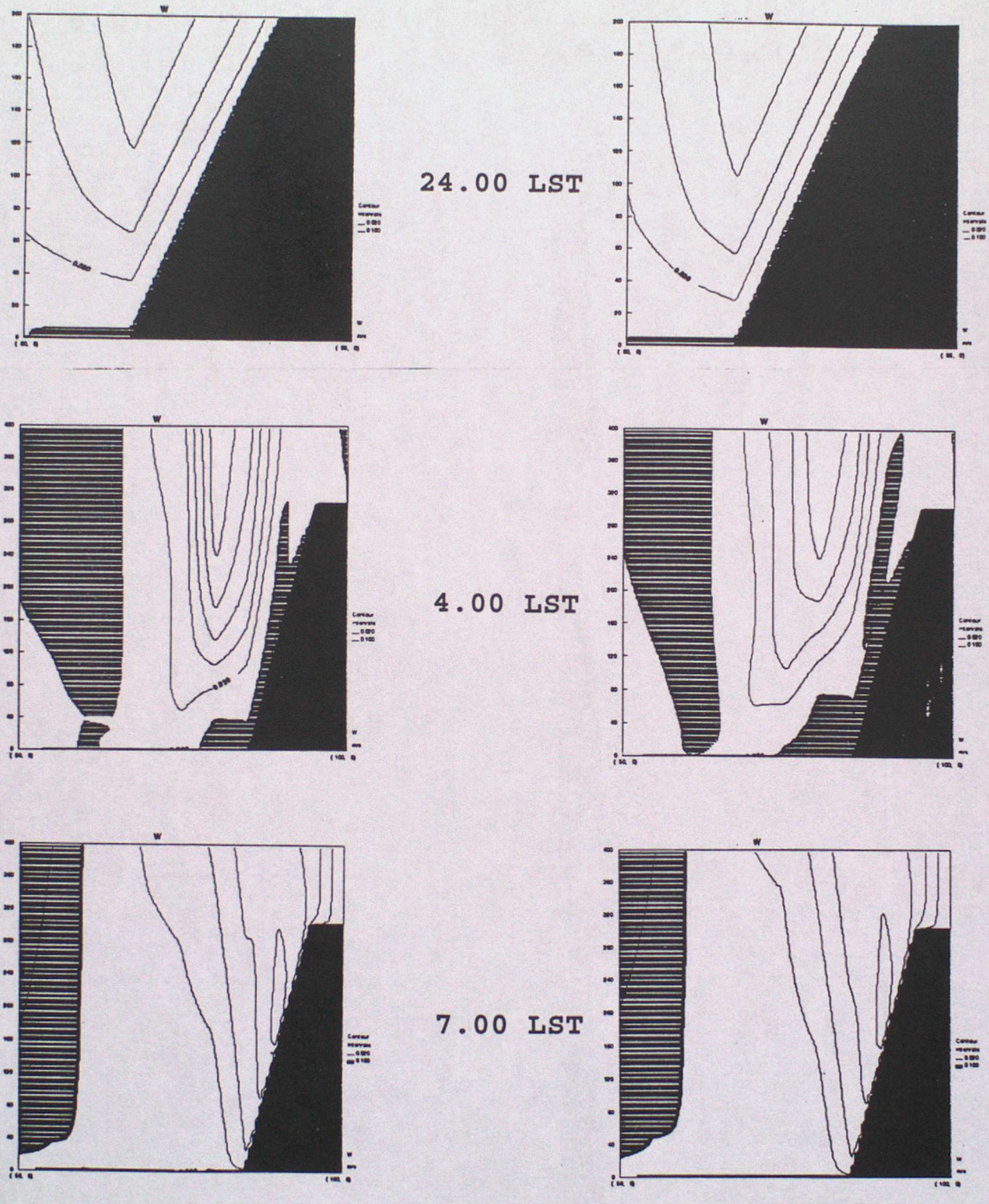

Fig.19. Evolution of the drainage flow. Shading denotes descent. (contour interval is 0.02 m/s). The plots at 24.00 are of a smaller area in order to render the drainage flow visible.

Small Scale Evolution of Potential Temperature.

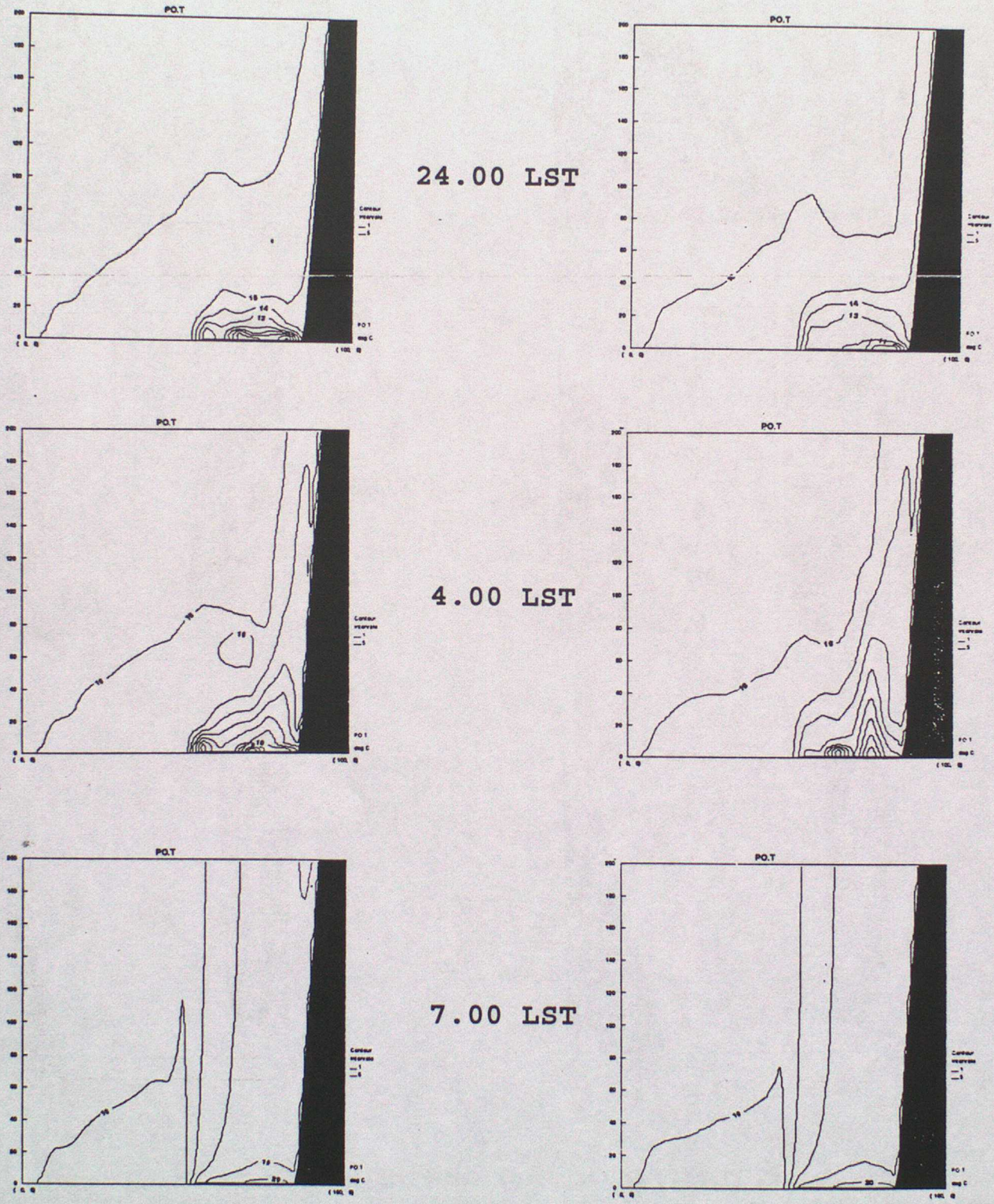

Fig.20. Evolution of potential temperature.

Small Scale Evolution of Relative Humidity.

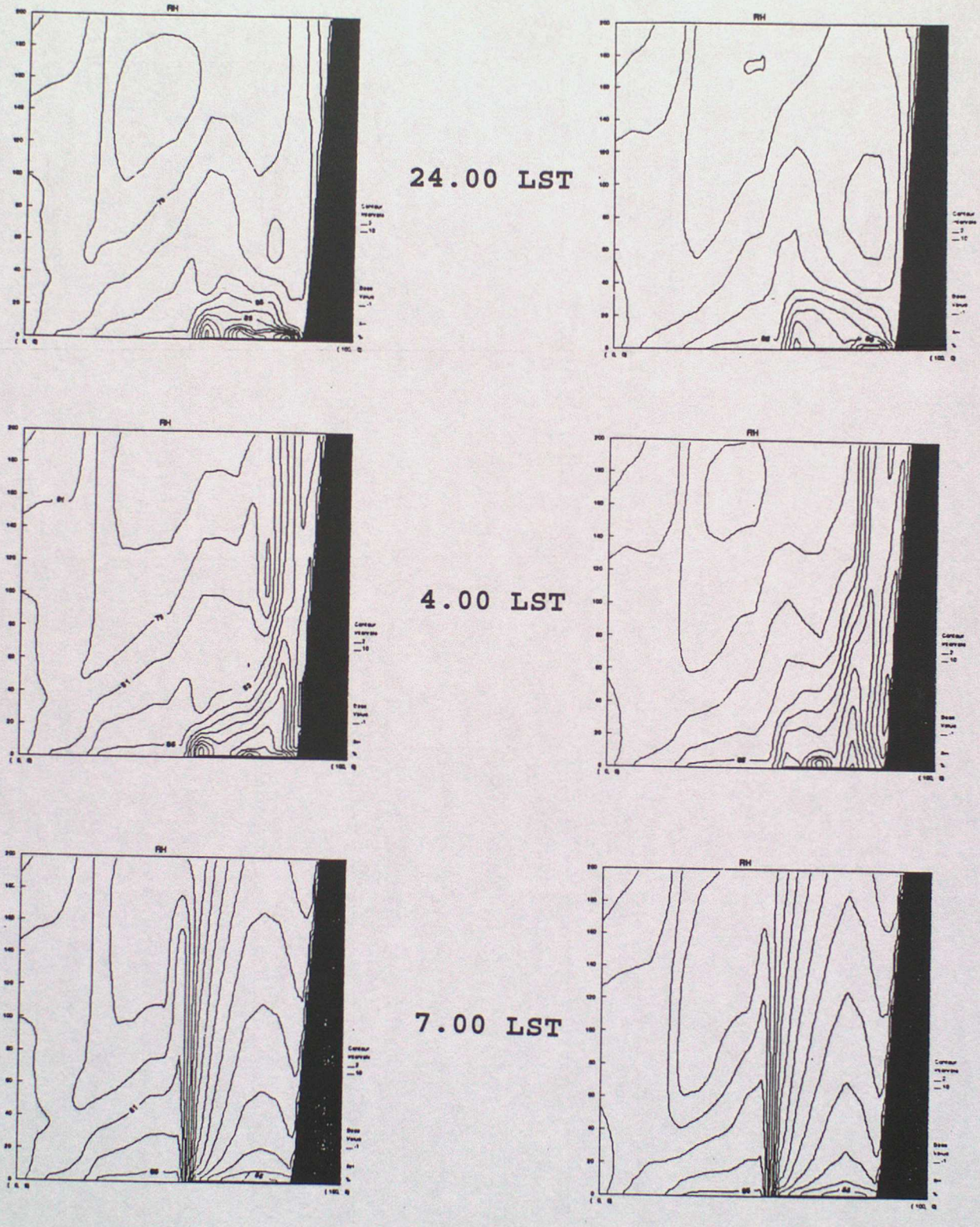

Fig.21. Evolution of relative humidity.

Vertical profiles from Wangara Experiment.

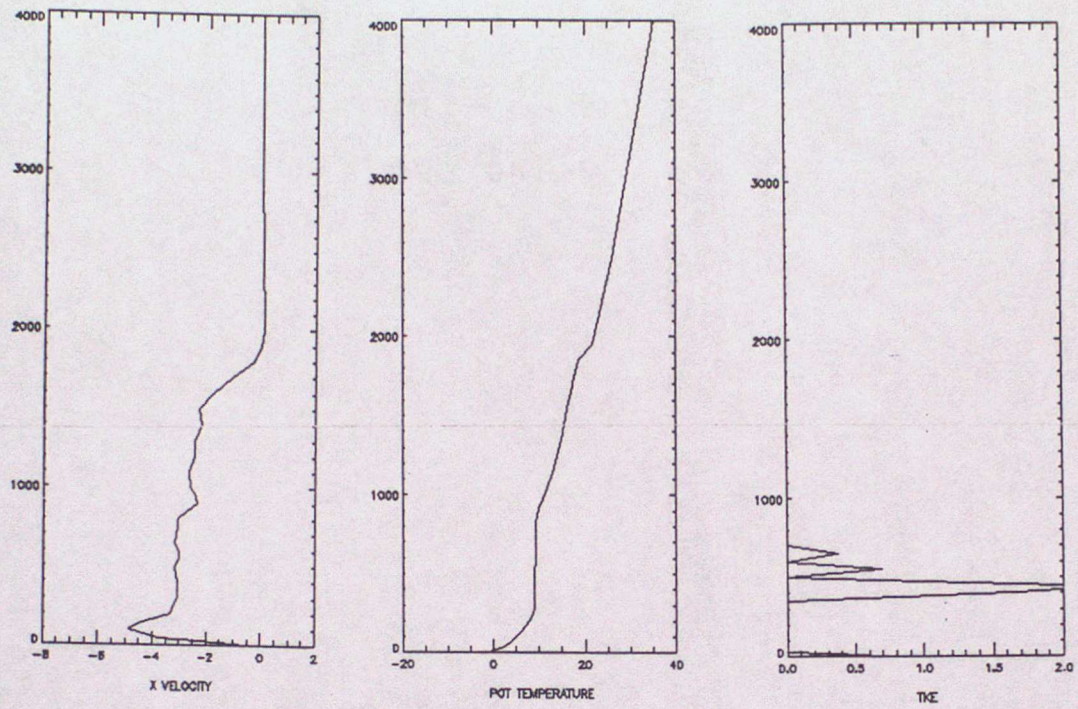

a) 0600 LST

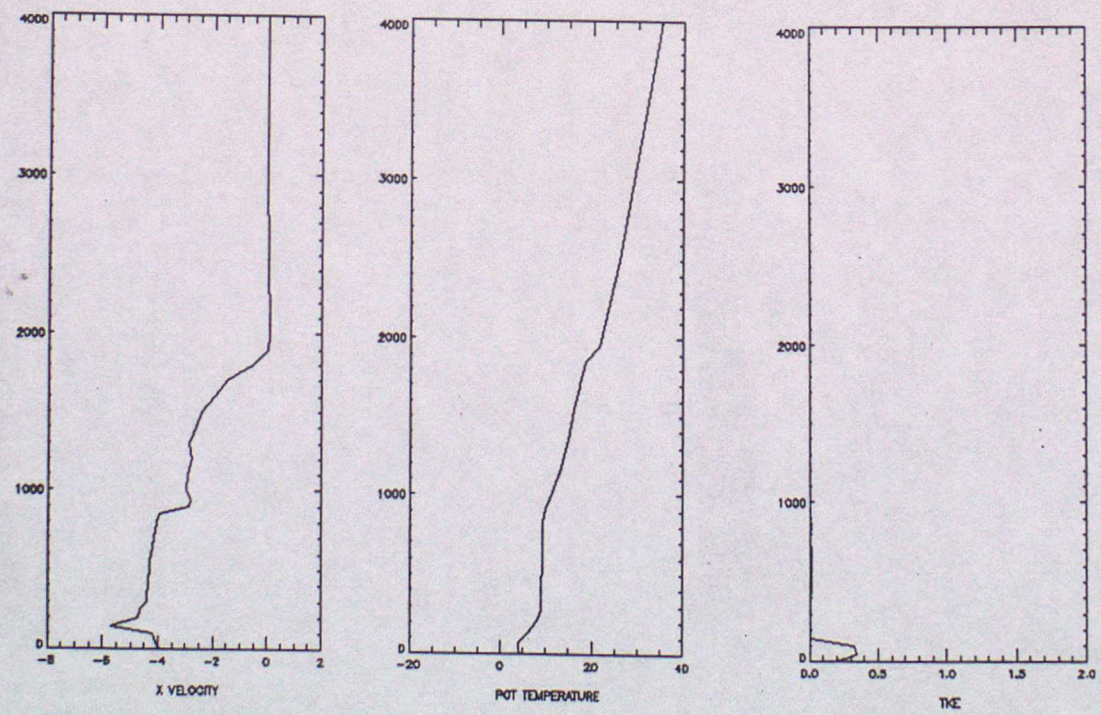

b) 0900 LST

Fig.22. Profiles of u, θ and TKE from the Lorenz grid model.

Vertical profiles from Wangara Experiment.

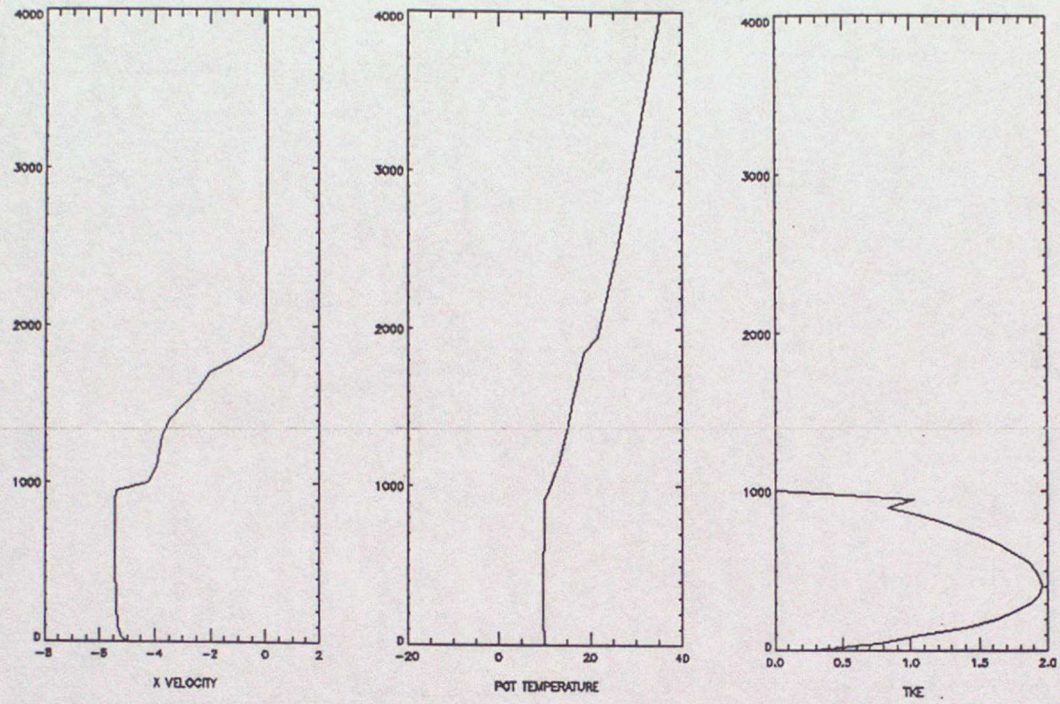

a) 1200 LST

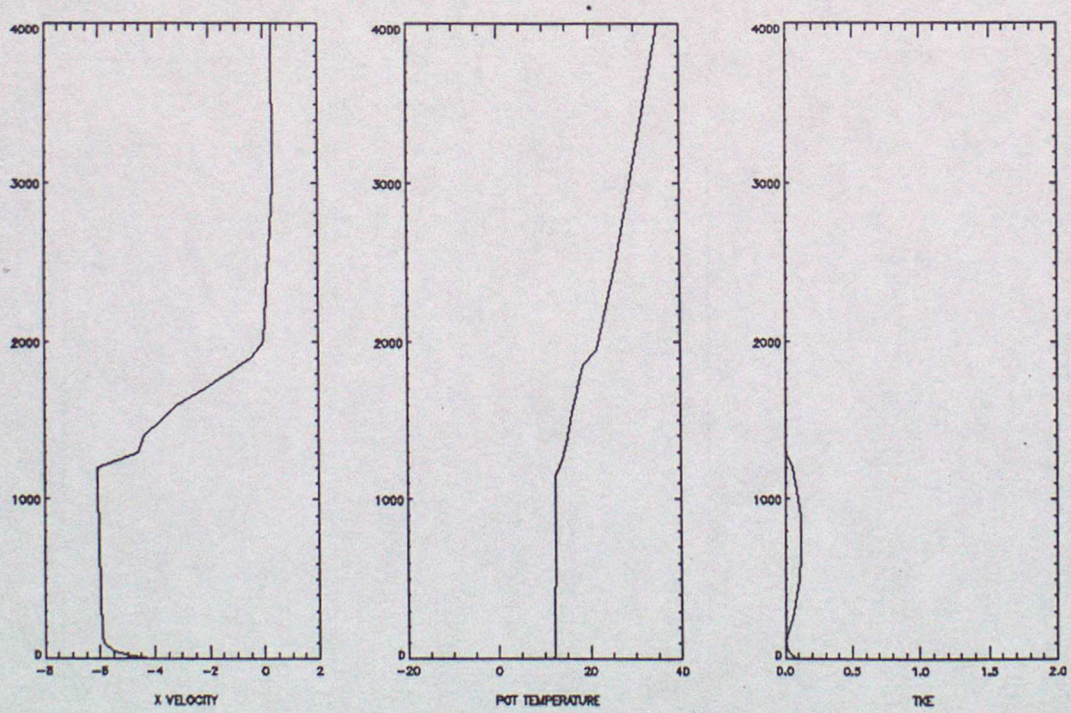

b) 1800 LST

Fig.23. Profiles of u, θ and TKE from the Lorenz grid model.

Vertical profiles from Wangara Experiment.

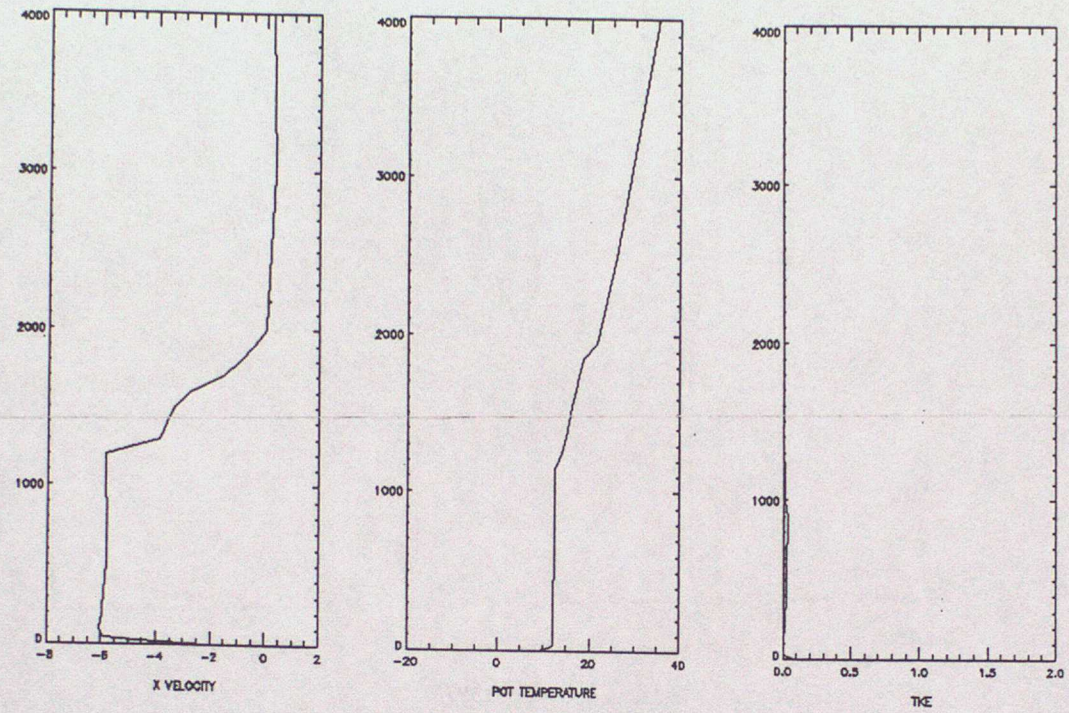

a) 2100 LST

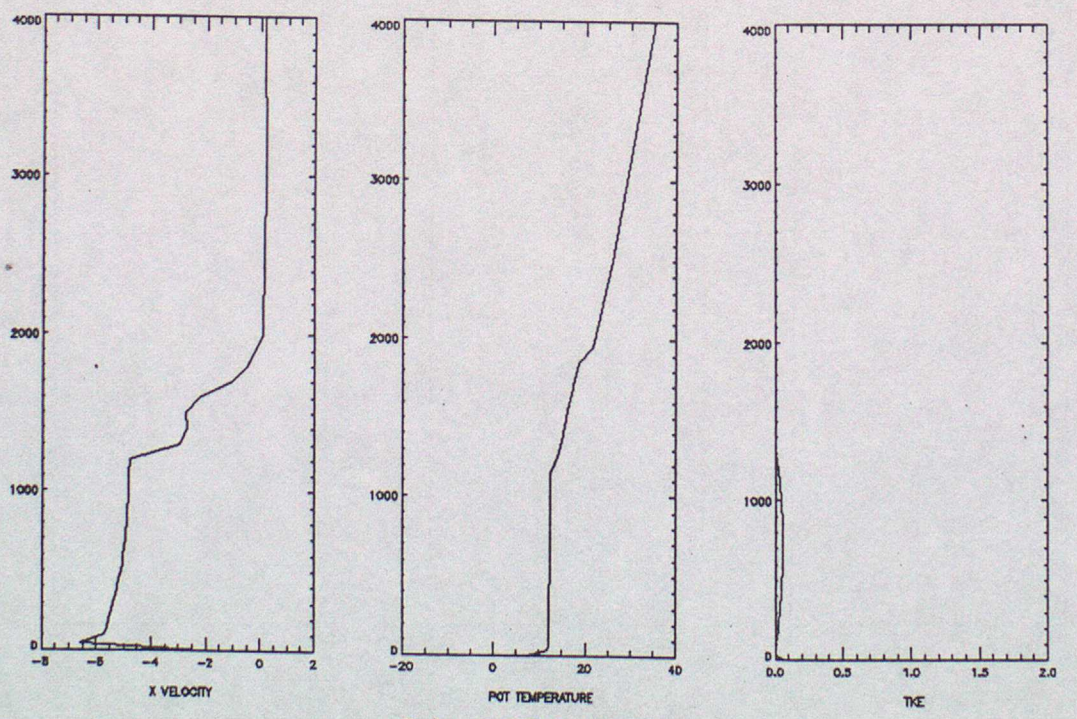

b) 2400 LST

Fig.24. Profiles of u, θ and TKE from the Lorenz grid model.

Vertical profiles from Wangara Experiment.

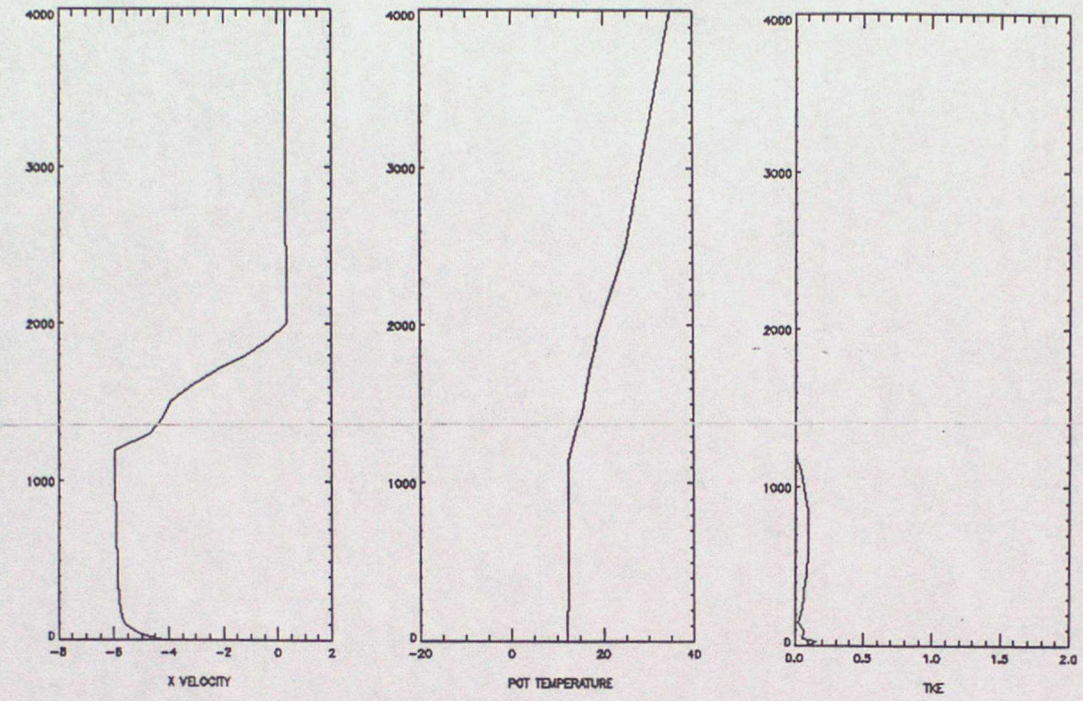

a) 1800 LST (u_bar)

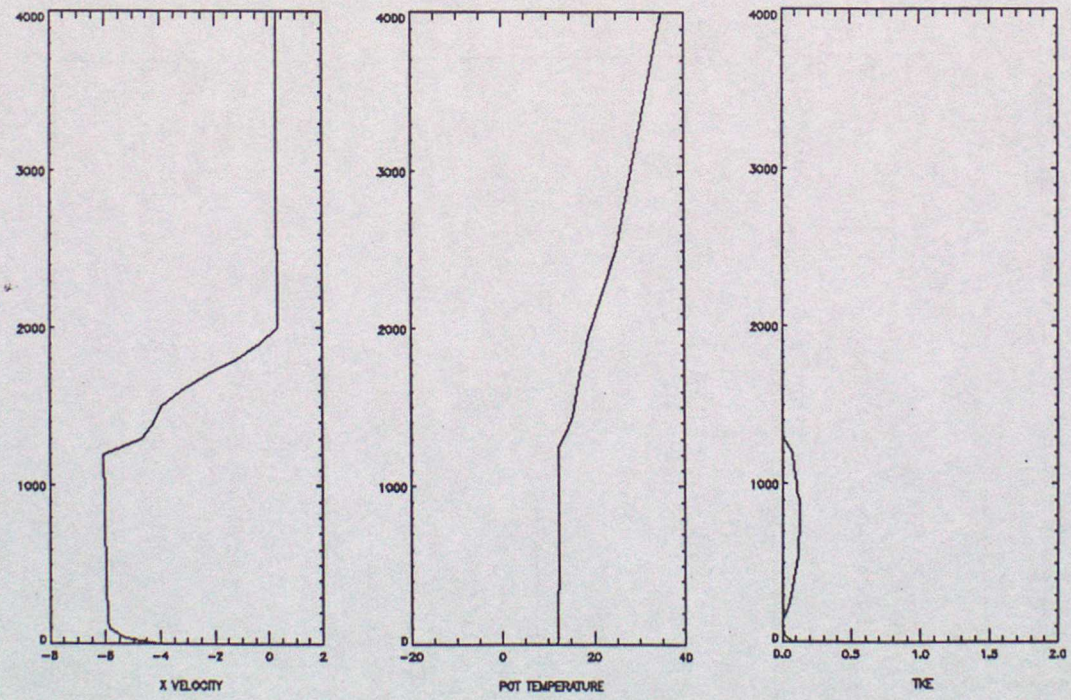

b) 1800 LST (θ_bar)

Fig.25. Profiles of u, θ and TKE from the Charney-Phillips grid model. For control run see figure 23b.

Vertical profiles from Wangara Experiment.

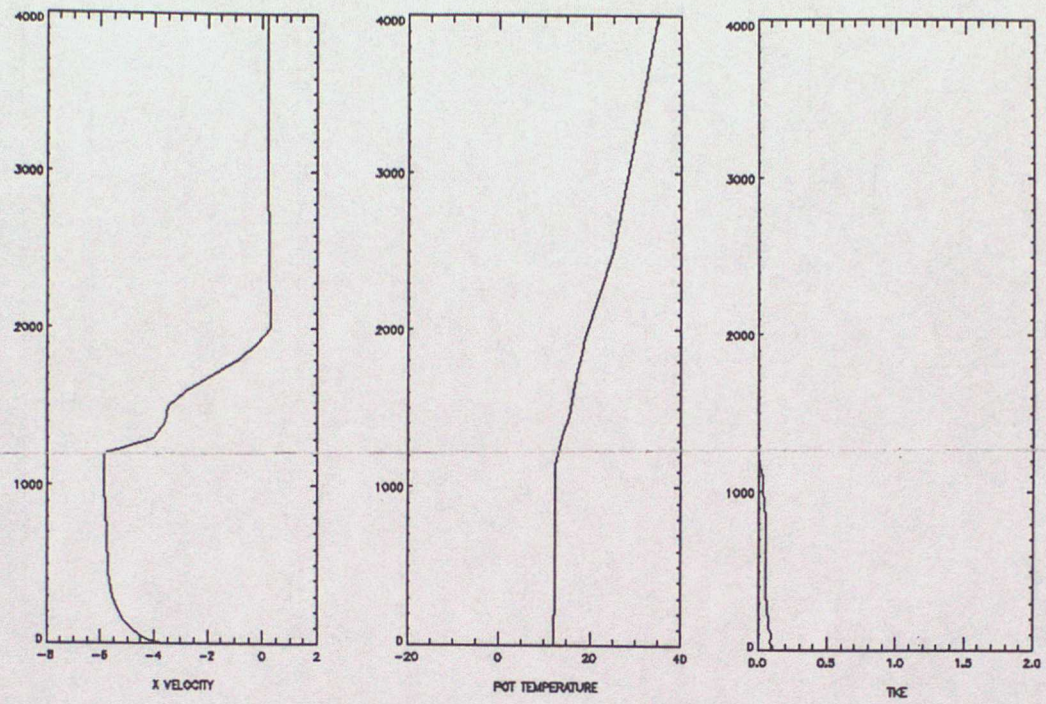

a) 2100 LST (u_bar)

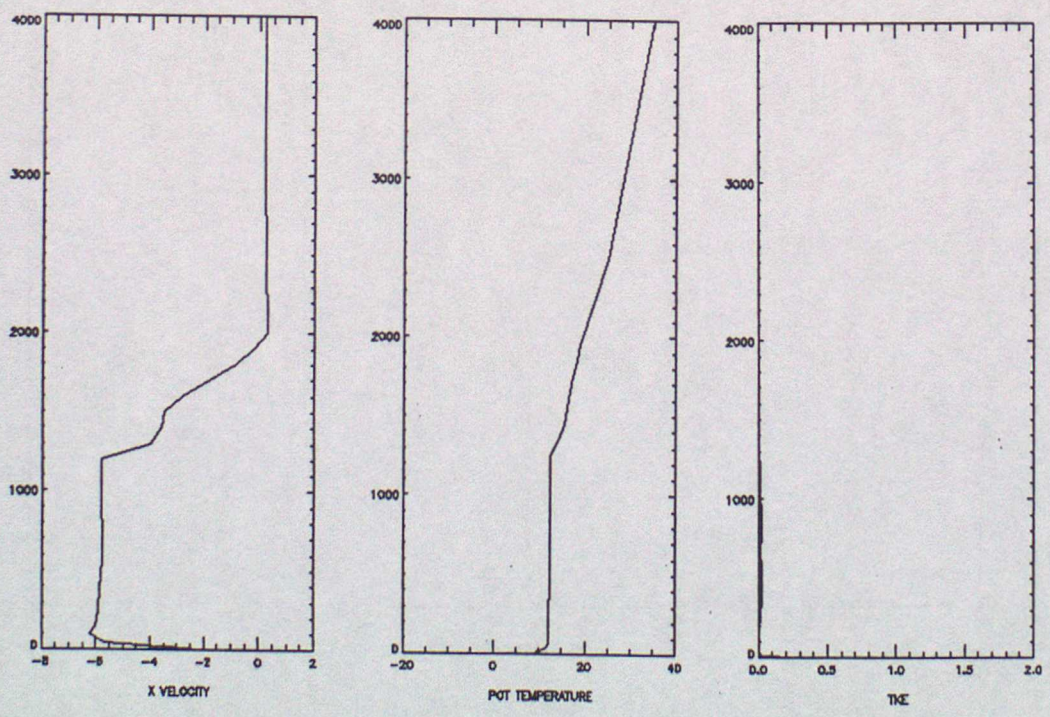

b) 2100 LST (θ_bar)

Fig.26. Profiles of u, θ and TKE from the Charney-Phillips grid model. For control run see figure 24a.

Vertical profiles from Wangara Experiment.

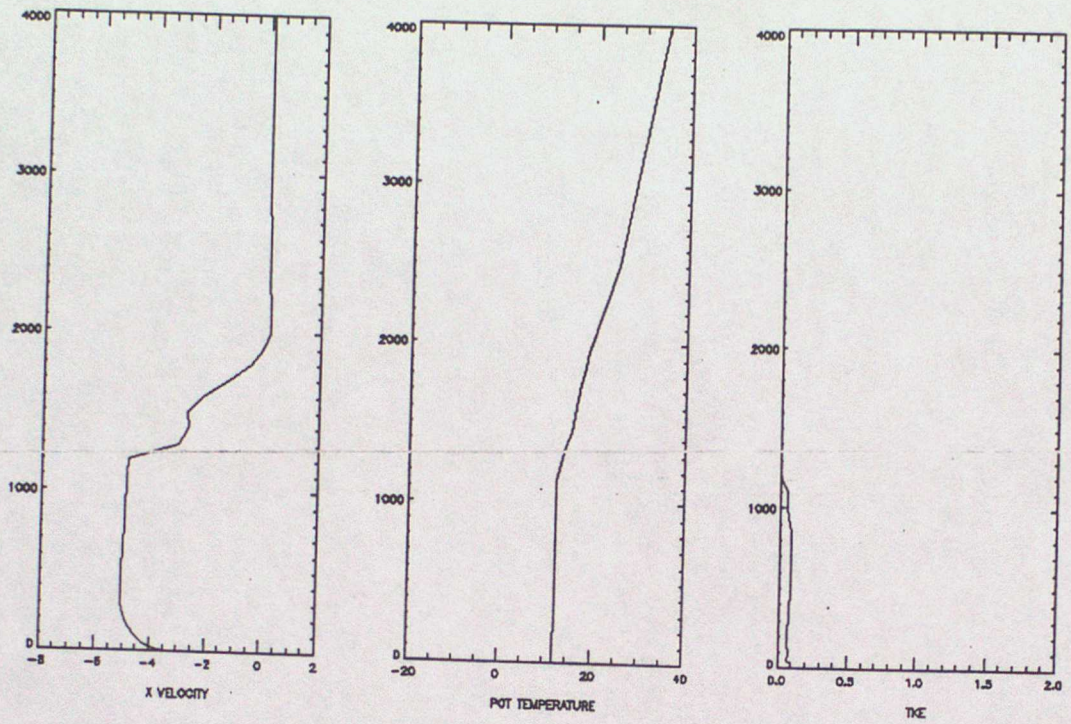

a) 2400 LST (u_bar)

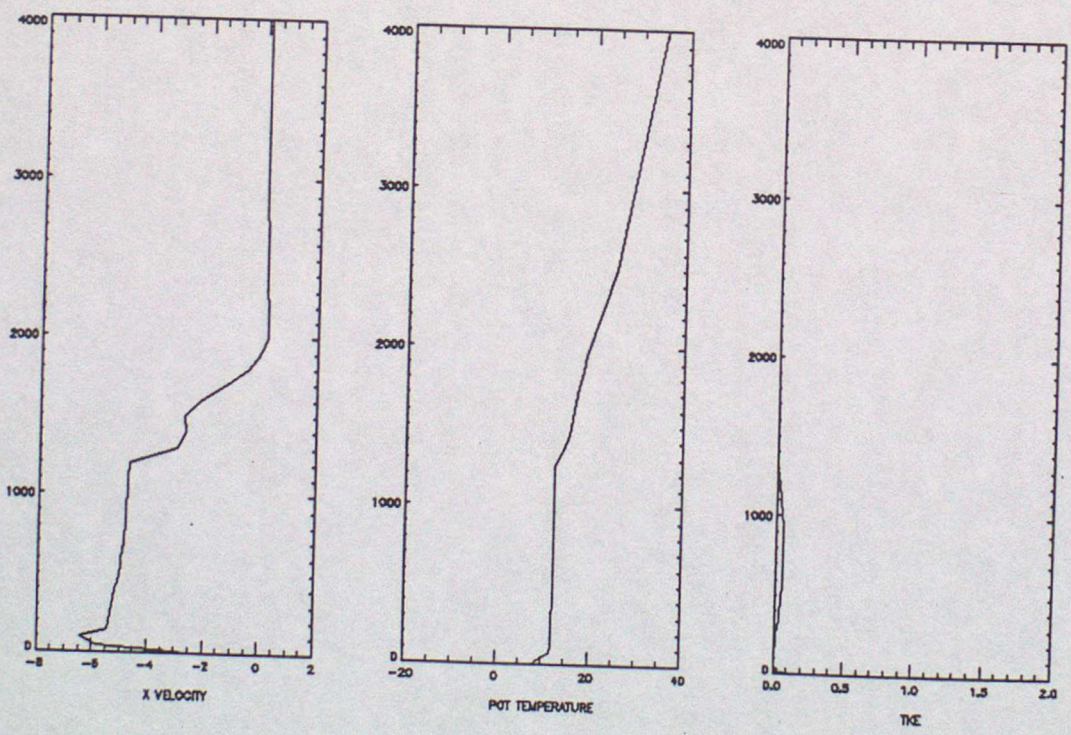

b) 2400 LST (θ_bar)

Fig.27. Profiles of u, θ and TKE from the Charney-Phillips grid model. For control run see figure 24b.